

# ASSIMILATION OF INFORMATION ON MOISTURE AND DIABATIC HEATING FROM SATELLITE IMAGERY

K. Puri, N.E. Davidson and P.J. Steinle

Bureau of Meteorology Research Centre  
Melbourne, Australia

## 1. INTRODUCTION

Diabatic processes play an important role in determining the circulation in the tropics. Current numerical prediction models have problems in adequately handling these processes for a number of reasons. These include sparsity of data, deficiencies in the parametrization of physical processes (particularly cumulus convection), failure of analysis schemes to include information on diabatic heating, and the inability to provide initial fields that are dynamically consistent and sensitive to regions of heating and cooling. These factors have a deleterious impact on model performance in the tropics and also result in a model spinup where the precipitation and evaporation take one or two days to reach equilibrium values.

One of the reasons for the poor representation of tropical diabatic forcing is sparsity of moisture data. Geostationary satellites such as the Japanese Geostationary Meteorological Satellite (GMS) provide useful proxy sources of moisture data. For example, the Japan Meteorological Agency (JMA) and the Australian Bureau of Meteorology (BOM) operationally derive moisture data from the GMS based on collocations between radiosondes and satellite radiances (See Baba, 1987 and Mills and Davidson, 1987), and the use of this data has been shown to be beneficial to model performance in the tropics.

An aspect of spinup in the tropics is the lack of consistency in the initial fields between the divergent circulation, diabatic heating and the moisture field. Although it is possible to define a balanced divergence field that is consistent with the diabatic heating using diabatic normal mode initialization (NMI) (See Wergen, 1987), the balance will be rapidly lost if the moisture field is not consistent with the diabatic heating. One way of overcoming this problem is to adjust the initial moisture field so that the precipitation in the early stages of the model integration is consistent with the heating rates used during diabatic NMI. Moisture initialization, which is also referred to as physical initialization, was introduced by Krishnamurti et al., (1984) and has also been used by Donner (1988), Puri and Miller (1990), Kasahara et al. (1992) and Puri and Davidson (1992).

In this paper the application and impact of the satellite based synthetic moisture data, diabatic heating and moisture initialization in the BMRC Global Assimilation and Prediction (GASP) system and the limited area Tropical Analysis and Prediction System (TAPS) is presented. Puri (1987) and Kasahara et al. (1988) carried out preliminary studies to use satellite data in numerical models for diabatic NMI and as a means of improving the divergent wind analysis in the tropics. As was noted earlier, the pioneering work on moisture initialization was carried out by the Florida State University (Tallahassee) group headed by Krishnamurti, who showed that it could have positive impact on simulating aspects of the Indian monsoon. Donner and Rasch (1989) performed a number of experiments with a global spectral model with synthetic diagnosed distributions of latent heat release and divergence obtained by integrating the model for three days prior to the initialization time of an experimental forecast. They showed that physical initialization of Donner (1988) can recover initial distributions of latent heating but that a further spinup (overshooting) still occurs. Turpeinen et al., (1990), in an attempt to alleviate the spinup problem in the Canadian regional finite-element model, used latent heating profiles directly in the model. The estimates of heating rates were based on precipitation rates inferred from Geostationary Operational Environmental Satellite (GOES) and infrared and visible imagery. They also enhanced the relative humidity fields to 95% wherever the probability of precipitation was larger than 40%. They showed that for the case of an extratropical storm the spinup time of vertical motion, initially of order of 9h, could be practically eliminated, although some short-lived spinup still occurred. Turpeinen (1990) further studied the dependence of spinup time on the initial humidity field, the vertical structure of the latent heating profile, and the precipitation rates used in initialization. His results indicate that diabatic initialization alone does not lead to any reduction in spinup if no humidity enhancement is applied where latent heat is released. Furthermore, he found that the results were not very sensitive to the accuracy of the specified rain rates, although the identification of rain areas is important. Puri and Miller (1990) applied the procedure of diabatic initialization using heating rates estimated from satellite-derived rainfall rates in the ECMWF data assimilation system and also developed a moisture initialization scheme based on the Betts-Miller (Betts and Miller, 1986) convection scheme.

The positive impact of the synthetic moisture data has been shown by the studies of Baba (1987), Mills and Davidson (1987) and Puri and Davidson (1992). More recently Davidson and Puri (1992) and Mathur et al. (1992) have studied procedures for assimilating diabatic heating information using dynamical nudging.

A brief description of the derivation of synthetic moisture and heating rates from the GMS imagery, moisture initialization, and GASP and TAPS is given in section 2. Results from various studies are

presented in section 3 followed by examples of practical operational applications in section 4. Finally conclusions are given in section 5.

## 2. DESCRIPTION OF SATELLITE DERIVED PRODUCTS AND MODELS

### 2.1 Generation of synthetic moisture data

Subjective interpretation of satellite imagery has for some years been an important component of the BOM objective analysis system (Guymer, 1978). The use of GMS imagery to deduce vertical profiles was pioneered at JMA where this synthetic data has been used operationally for several years (Baba, 1987). A simplified version of the JMA scheme has been developed at BMRC by Mills and Davidson (1987) and a brief description of this scheme will be presented.

The premise on which the development of the moisture retrieval algorithm was based was that a statistical analysis of the equivalent black-body temperature of each pixel (which will be regarded as the cloud top temperature, CTT) in an area co-located with a radiosonde ascent could be used to classify the cloud depth, amount and type in that area, and that this cloud classification could be related to the dew-point depression profile of the associated radiosonde ascent.

The development of the Mills and Davidson (MD) scheme involved comparing the CTT of each pixel within a 50 km radius circle surrounding each radiosonde site with the temperatures at the fixed location as interpolated from the BOM archived objective analysis. The cloud top, as represented by the CTT of that pixel, was then assigned to be within one of the layers defined by the analysis pressure levels, i.e. to the layers surface-850hPa, 850-700hPa, 700-500hPa, 500-300hPa, and above 300 hPa. For each layer and for the whole troposphere, the fractional pixel count (i.e. the cloud amount), the mean CTT, and the standard deviation of CTT of the cloudy pixels within that layer were then determined. This provided a data set of CTT statistics and co-located radiosonde dew-point depression profiles on a monthly basis for one calendar-year, containing some 8500 items. Rather than derive statistical regression relationships between the cloud and radiosonde observations, the data were stratified into categories based on three a priori criteria. The first classification criterion was the layer of maximum cloudiness, the second was whether the cloud amount in the layer covered more or less than 50% of the area, and the third was whether the major cloud layer was cumuliform or stratiform. This final cloud-type assignment was based on the standard deviation of the CTT within the layer, with a standard deviation greater (less) than 3.5° C indicating cumuliform (stratiform) cloud. If the layer of maximum cloudiness was below 850hPa, no cumulus category was assigned and if cloud

amount was less than 20%, the sounding was designated 'clear'. Accordingly 19 categories were assigned: amount (scattered, broken) by depth (5 layers) by type (cumuliform, stratiform), plus one 'clear' category, less two categories since no cumulus category was assigned below 850hPa.

The dew point profiles associated with each of those 19 categories were then averaged to provide a mean dew-point depression profile from 850 hPa to 300 hPa per each category. The data was stratified into summer (October-March) and winter (April-September) classification, but very little difference was found between the two. Fig. 1 (taken from Mills and Davidson, 1987) shows the annual mean dew-point depression profiles for each of the 19 cloudiness categories together with the corresponding cloud classification and the top of the layer of maximum cloudiness. In general terms, the profiles seem compatible with their cloud groups: moisture is greater below cloud top level, there is more moisture for broken than for scattered cloud categories, and there is more lower (upper) level moisture for cumuliform (stratiform) categories.

The practical application of the system involves the following steps.

- (i) Ingestion of satellite pixel data
- (ii) For 50 km radius circle on a latitude-longitude grid covering the satellite image, compute mean CTT, the fractional pixel count (i.e. cloud amount) and the standard deviation of the CTT of the cloudy pixels within the layer (type of cloud).
- (iii) The assignment of the corresponding cloud category and dew-point depression profile at each of these points.
- (iv) Recover dewpoint using current temperature analysis if available or from 24 hours prior to satellite base time if current analysis is not available. In the latter case the moisture data is later checked by comparing the used temperature analysis with actual analysis and eliminating those observations where there are discrepancies between the two.

Moisture profile data are currently operationally generated four times per day on a  $2^{\circ} \times 2^{\circ}$  latitude-longitude grid over the domain covered by the GMS. The generated data are then treated as observations and used operationally in TAPS. A typical coverage of the conventional and synthetic moisture observations at 850 hPa is shown in Fig. 2.

Some of the known deficiencies of the moisture data include -

- (i) There is no stratification of data in space. Thus, the essentially extratropical data is also used in the tropics.

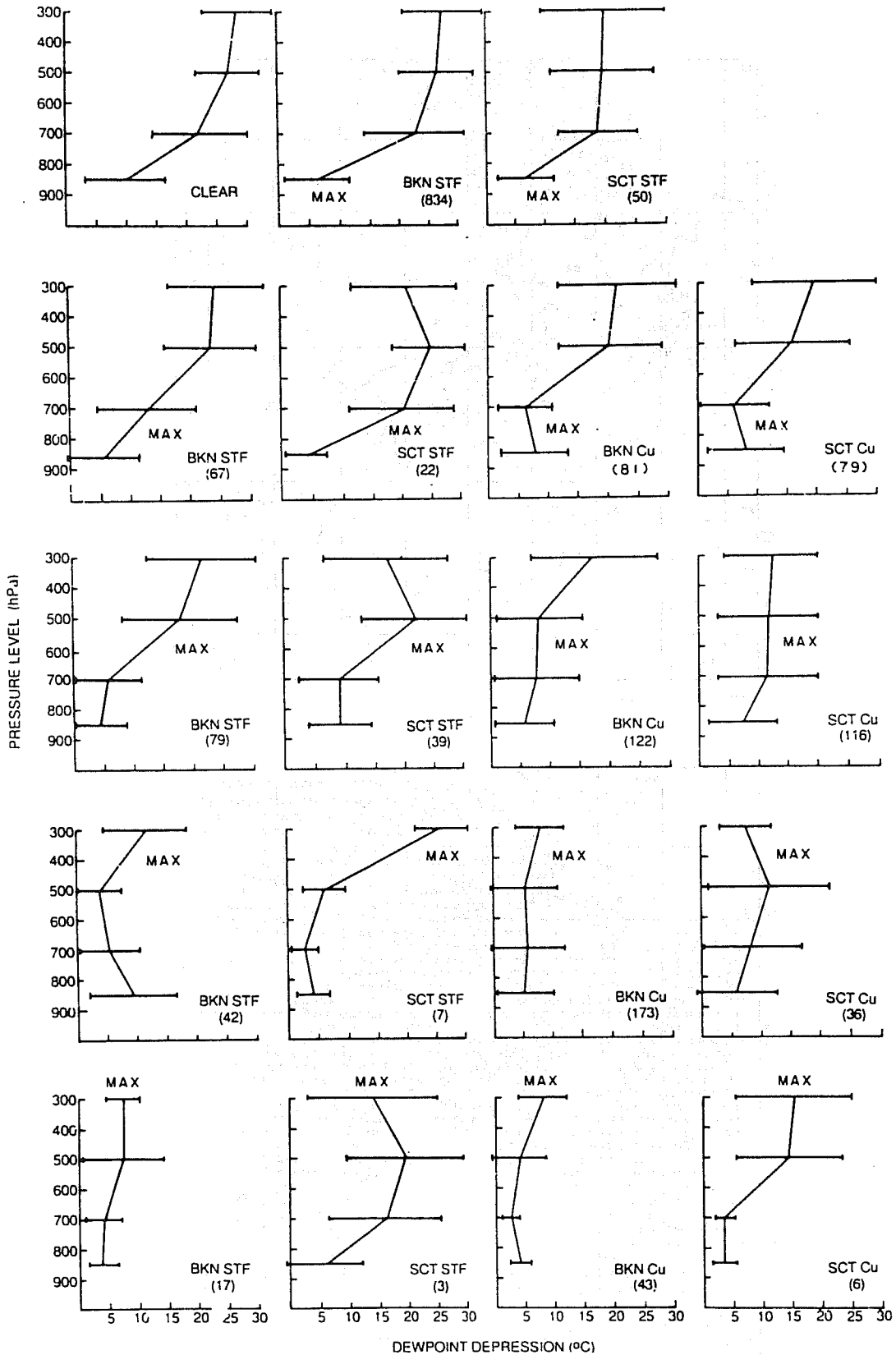
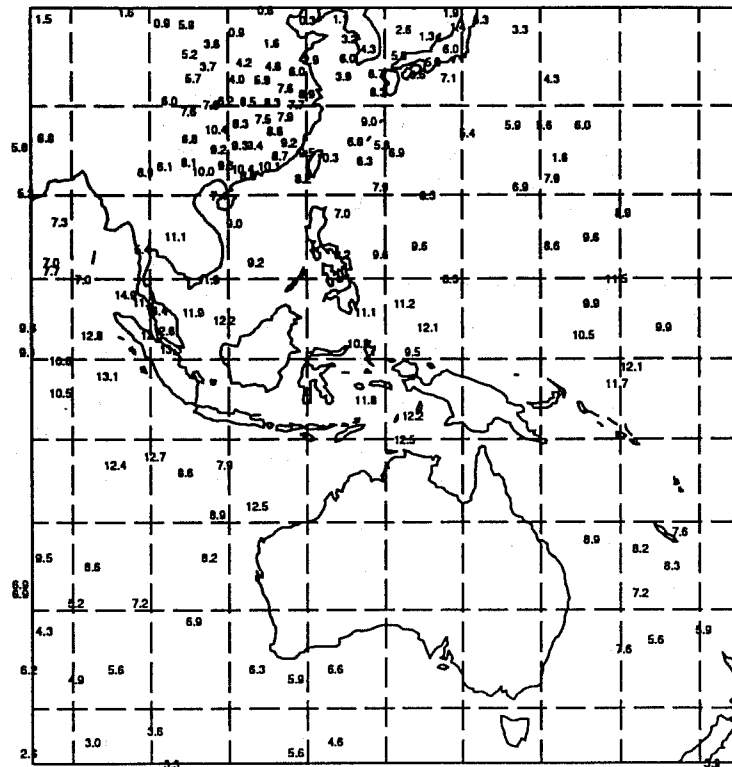
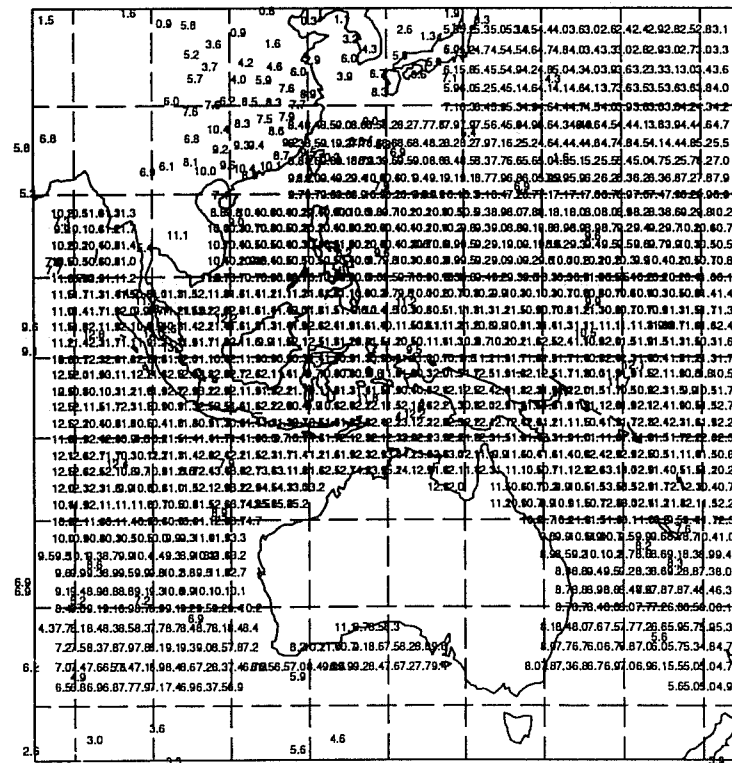


Fig. 1 Dew-point depression profiles for each of the 19 cloud categories, together with the type of cloud (cumuliform (Cu) or stratiform (STF)) whether greater (BKN) or less (SCT) than 50% cloud cover. Bracketed numbers indicate the number of matchups in each category, while 'MAX' indicates pressure layer in which the maximum cloud amount resides.



MIXR 920301 1100 850 MB



MIXR 920301 1100 850 MB

Fig. 2 An example of conventional (top) and bogus moisture (bottom) observations available in real time.

- (ii) The variance of matchups is large in no-cloud areas including areas above low level cloud decks. Data in these regions could easily be left out or assigned lower weight in the analysis.
- (iii) The developmental data set on which the statistics were based was biased towards stations with a maritime climate and thus the profiles cannot adequately represent the low level dryness found over the inland of large continents. Thus the data is not used below 850hPa over land.
- (iv) The data is currently generated on a  $2^{\circ} \times 2^{\circ}$  grid. The resolution can be easily increased if needed.

It should be noted that the JMA scheme is more comprehensive than the MD scheme. It uses SYNOP observations in addition to the GMS cloud data so that the latter provides information from above the clouds while the SYNOP observations provide information from below. The use of both types helps increase the reliability of the classification of the cloud conditions. The JMA scheme also divides the cloud conditions according to the latitude of the data into the tropical group ( $23.5^{\circ}\text{N} - 23.5^{\circ}\text{S}$ ) and the subtropical group ( $50^{\circ}\text{N} - 23.5^{\circ}\text{N}$ ;  $23.5^{\circ}\text{S} - 50^{\circ}\text{S}$ ). This division enables a distinction to be made between the relatively dry atmosphere in the middle latitudes and the moist tropical atmosphere. The total number of cloud categories in each group is 141. Comparison of the MD profiles with the JMA counterpart shows reasonable agreement. The main difference is in the layer below 850hPa where the dewpoint depressions from the JMA system are around  $2^{\circ}\text{C}$  less (more moist) than those from the MD system.

## 2.2 Estimation of heating rates

The commonly used procedure of applying model generated heating rates during diabatic NMI (see Wergen, 1987 for example) can lead to problems arising from deficiencies in the parameterization of convective processes and analysis of divergence and moisture fields; for example, the heating rates might be too weak or convective processes might occur at incorrect locations. Although no procedure exists as yet for directly measuring heating rates, satellite measurements of outgoing long wave radiation (OLR) provide indirect and approximate information for this quantity.

Puri and Miller (1990) have considered two procedures for estimating heating rates. Both rely on first obtaining estimates of rainfall rate  $R$ , which is essentially a measure of the vertically integrated heating rate at a particular location. In the first method the vertical profile is specified based on observations of typical profiles in convective situations, and the intensity can then be readily evaluated. An example of the profile used in TAPS is shown in Fig. 3 (taken from Davidson and Puri, 1992) together with profiles deduced from experimental data sets. The use of the same specified vertical profile

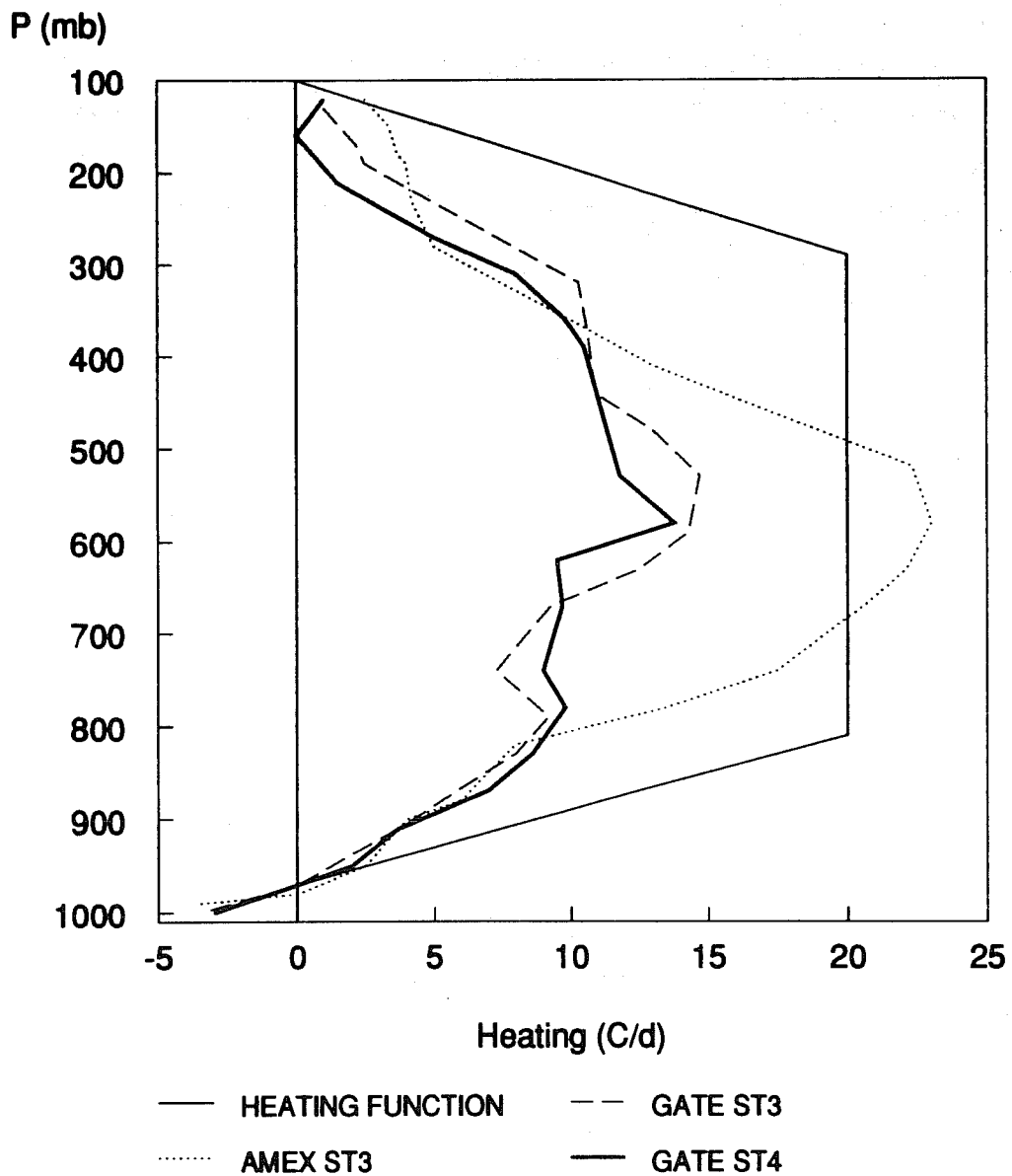


Fig. 3 Vertical profile of imposed heating for deep convection, and diagnosed heating rates ( $^{\circ}\text{C day}^{-1}$ ) from special experimental data (Frank and McBride, 1989).



throughout a particular domain is unsatisfactory, however, because 1) observational evidence indicates that profiles can vary with location, 2) profiles can vary according to the stage in the life cycle of a convective system, and 3) the specified profile may not be consistent with the parameterization used in the model. It is possible to overcome these problems by deriving the heating rates from the convective parameterization used in the model. For the Kuo parameterization, given  $R$ , the moisture convergence is set to  $R \times 2\Delta t$  (the factor 2 is to allow for the leap frog time-stepping scheme in the BMRC models), where  $\Delta t$  is the model time step and the moistening parameter is set to 0. The scheme will now generate a heating rate that is consistent with both the Kuo parameterization and rainfall data. This latter procedure, however, has a potential shortcoming that it is only possible to apply heating rates at points where the model diagnoses convection. The scheme cannot adequately handle points where observations indicate convection, but the model does not. An additional disadvantage is the profiles from the Kuo scheme may not be consistent with the 'real' profiles.

Once the heating rates are known, they can be readily used either through diabatic NMI or diabatic dynamical nudging. The latter has some advantages and will be considered in more detail in section 3.4.

### 2.3 Moisture initialization

The moisture initialization used here is based on the Betts-Miller parameterization and has been described in Puri and Miller (1990) and the interested reader is referred to the paper for details. The scheme attempts to adjust the initial moisture field so that the rainfall rate in the early stages of the model integrations ( $R_m$ ) is close to the observed rate ( $R$ ). If  $\delta q$  denotes the moisture adjustment, then in practice the following combinations can occur:

- (a)  $R_m > R$  then  $q_a = q_i - \delta q$   
 $R_m < R$  then  $q_a = q_i + \delta q$ ,

where  $q_i$  and  $q_a$  are the unadjusted and adjusted moisture fields respectively;

- (b)  $R_m = 0$  i.e. no convection diagnosed by the model and  $R > 0$ . The scheme cannot cope with this, and no adjustment is made to the moisture field.

Some of the notable features of the scheme are as follows:

- (i) Only the moisture field is modified and the temperature is left unchanged  
(ii) The observed rainfall is assumed to be convective rainfall

- (iii) The scheme is only applied in the tropics
- (iv) The moisture adjustment will only occur in regions where convection is diagnosed in the model. One possible way of overcoming this limitation would be to modify the temperature field so that the relevant layer or layers become convectively unstable. The temperature analyses, however, are much more reliable than moisture analyses, and it is preferable not to modify the temperature during initialization.

Krishnamurti et al. (1984), Donner (1988) and Kasahara et al. (1992) have applied moisture initialization in conjunction with the Kuo convective parameterization.

### 3.4 Description of analysis-forecast systems

Both the Global Assimilation and Prediction (GASP) system and the Tropical Analysis and Prediction System (TAPS) have been used for the results to be described in the next section. A detailed description of GASP has been given by Bourke et al. (1990). The prediction model is a global spectral model that has nineteen sigma levels in the vertical and is truncated at wave number 31 (rhomboidal truncation). The analysis component uses multivariate statistical interpolation (MVISI) with detailed quality control procedures. A Cressman type scheme is used for moisture analysis. GASP uses a 6 hourly intermittent data assimilation cycle.

A description of TAPS is given in Puri et al. (1992). The prediction model is a limited area finite difference model covering the domain 45°S - 40° N; 85°E - 180°E. The prediction model has nineteen sigma levels in the vertical (same as in GASP) and horizontal resolution of 95 km. The analysis component uses two dimensional statistical interpolation for all fields with variational blending of the mass and windfields. The boundary conditions for TAPS are obtained from GASP. No data assimilation is performed; the GASP fields are used to perform a reanalysis on the model grid.

Both systems use the same parameterization of physical processes. These include the constant flux layer which is parameterized by using the Monin-Obhukov formulation in which the drag coefficient is a function of stability near the surface. The vertical eddy transport in the free atmosphere is parameterized using the mixing length formulation in which the mixing lengths are stability dependent. Kuo cumulus convection parameterization is used with large scale condensation applied if the relative humidity exceeds a specified threshold. A separate shallow convection scheme (Tiedtke, 1987) is used to simulate transport of heat and moisture by low-level non-precipitating clouds. Ground hydrology and heat conduction through the soil are also included. The Fels-Schwarzhopf scheme (Fels and Schwarzkopf, 1975) is used to parameterize radiative transfer and diurnal variation is included. Cloud

amounts and heights are diagnosed using appropriate model variables (Rikus, 1991).

Some novel features of TAPS include the extensive use of satellite data described above and the use of diabatic dynamical nudging. The nudging scheme is used to provide a means of including information on diabatic heating in the initial state and to provide a balanced initial condition (Davidson and Puri, 1992). A schematic of the scheme as used in TAPS is shown in Fig. 4. A target analysis for nudging is first obtained from a reanalysis of all observational data including synthetic moisture and TC data. From 12 to 24 hours prior to the base time of the forecast the prediction model is nudged towards the target analysis and the 'observationally reliable' rotational wind component is preserved. During nudging the convective heating from the cumulus convection parameterization used in the model is replaced by heating determined from the GMS cloud top temperature data. This effectively replaces the divergent wind component in the target analysis. Nudging of the surface pressure and temperature is also necessary to adequately preserve the mass field over the limited area of the model. The moisture field is not nudged in order to allow it to come into balance with the improved heating and vertical motion fields. The perceived benefits of diabatic nudging are that it reduces model spin up time, enhances short term rainfall prediction and improves mass-wind balance and model acceptance of imposed synthetic tropical cyclone structures.

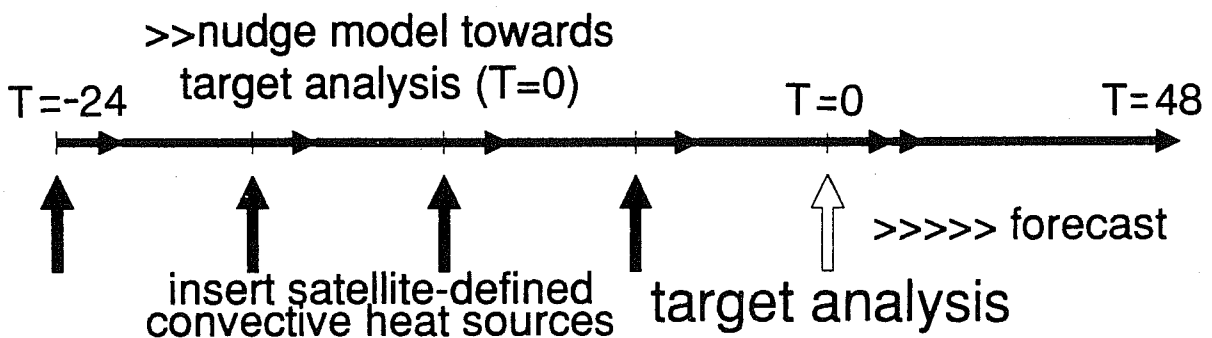
### 3. RESULTS FROM VARIOUS STUDIES

As was noted above, work on the assimilation of moisture and diabatic heating from satellite imagery is being carried out at a number of Centres. However, in the interest of brevity attention will be focussed here on the work being carried out at BMRC.

#### 3.1 Impact of GMS-based moisture data and diabatic heating in data assimilation

A number of data assimilation experiments (reported by Puri and Davidson 1992) were performed with an earlier version of GASP to that described in section 2.4. In this version a nine level model was used and the analysis component used univariate statistical interpolation. The diagnostic cloud option was not used and cloud amounts and heights were fixed zonal averages for each season using climatology of London (1957). The period chosen for the experiments was from 1100 UTC 11 January 1990 to 1100 UTC 16 January 1990. This period had significant convective activity in the tropics to the north of Australia and included three tropical cyclones, namely, Koryn in the central Pacific, Sam off the coast of northwest Australia, and Rosita in the central Indian ocean. An example of these systems can be found in the satellite imagery in Fig. 5. The following data assimilation

# DYNAMIC NUDGING OF THE BMRC TROPICAL PREDICTION MODEL USING SATELLITE-DEFINED CONVECTIVE HEAT SOURCES AND A CYCLONE BOGUS



- >> target analysis : re-analysis of all data + TC bogus + satellite moisture data; first guess from global 4-D assimilation system.
- >> nudge to preserve the observationally-reliable rotational wind component in the target analysis.
- >> replace Kuo heating during nudging with satellite-defined heat sources, updated every 6 hours (forces divergent wind component).

Fig. 4 A schematic of the dynamic nudging scheme used in TAPS.

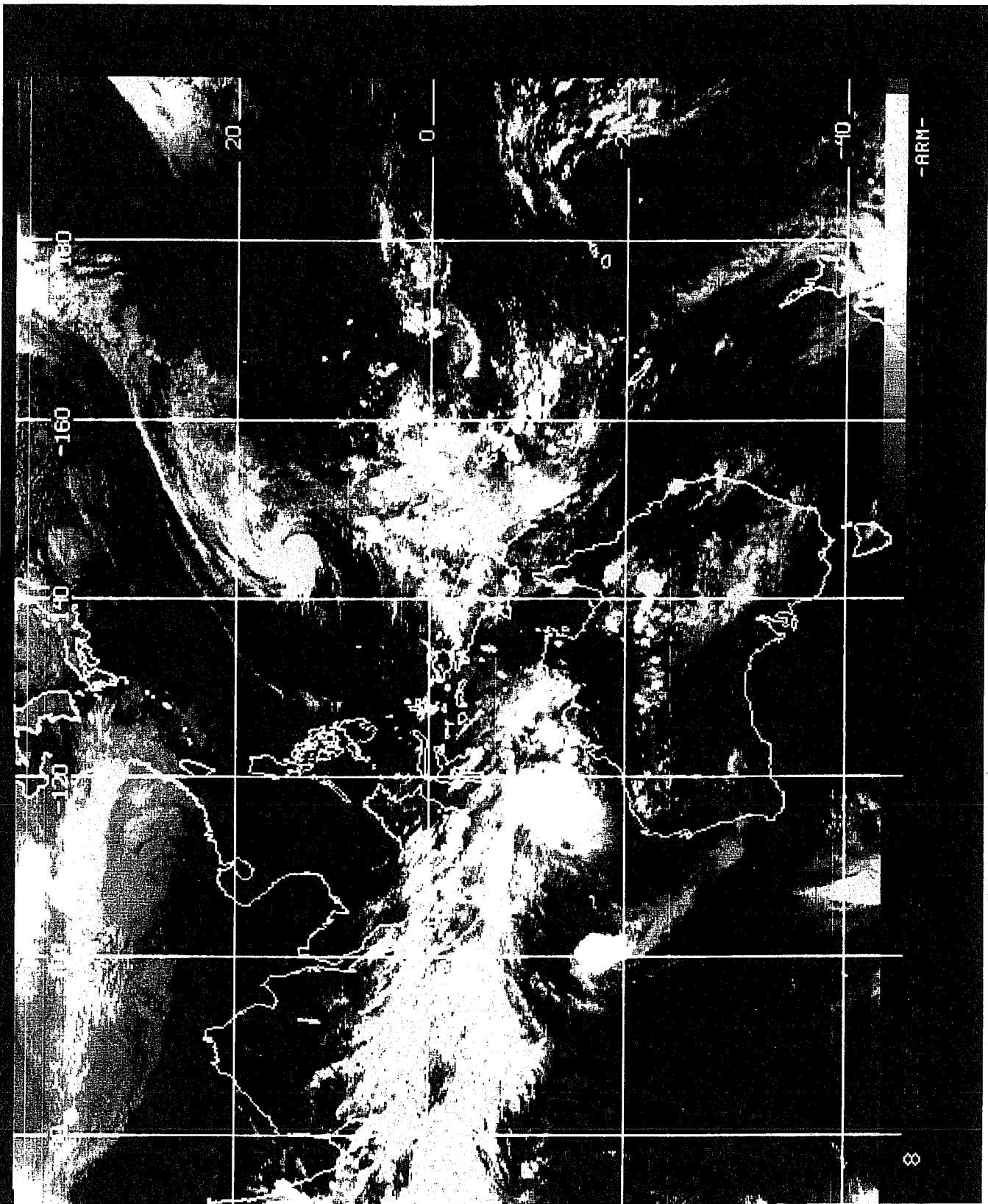


Fig. 5a GMS infrared imagery for 1100 UTC 14 January 1990.

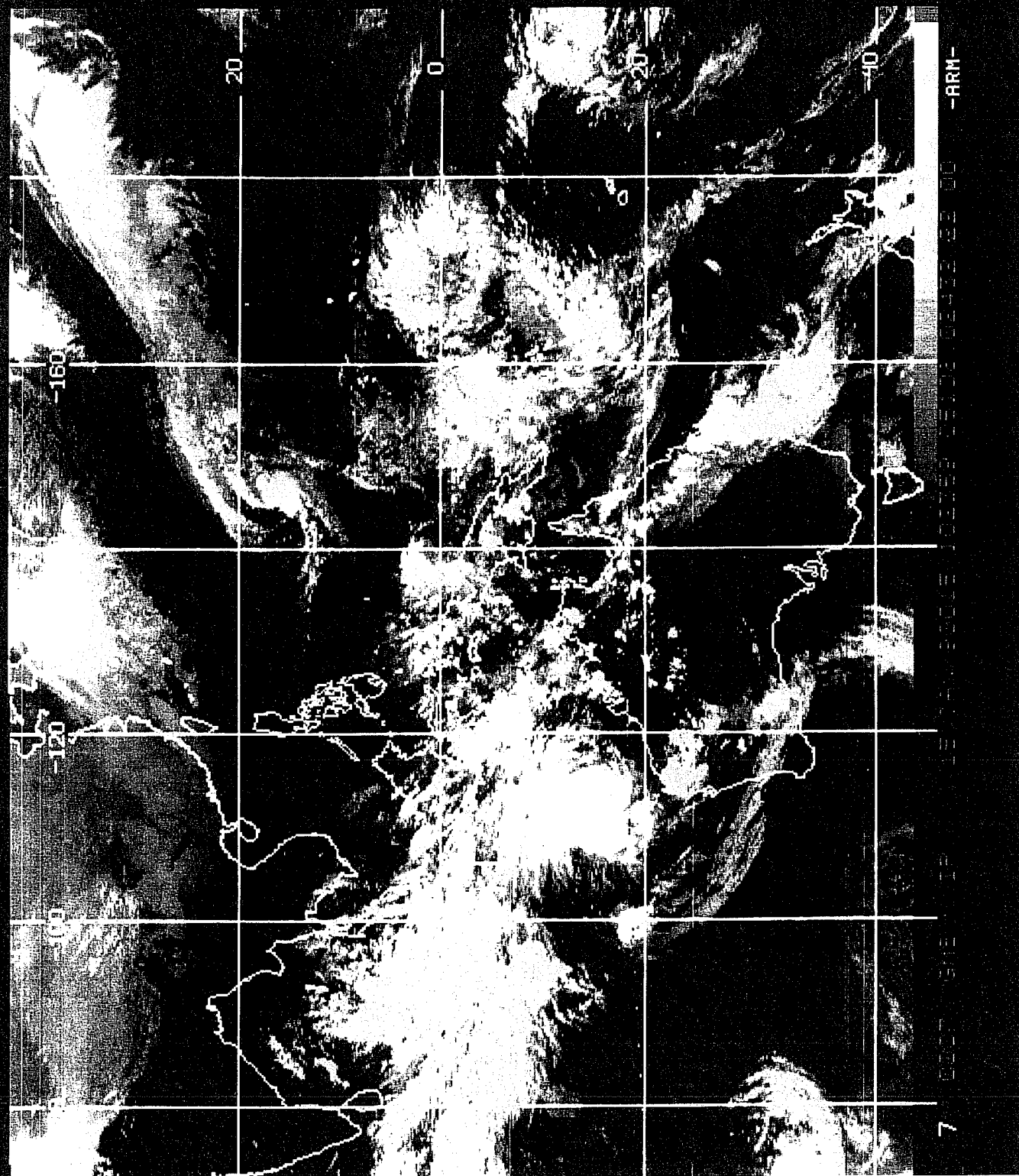


Fig. 5b As in Fig. 5a but for 1100 UTC 15 January 1990.

experiments were performed:

- CNTL: Control
- GMSQ: CNTL + synthetic moisture data at 1100 and 2300 UTC
- GMSI: GMSQ + diabatic NMI with heating rates estimated from GMS cloud top temperatures, and
- GMSH: GMSI + heating rates specified during the first 2h of model integration during the data-assimilation cycle.

In CNTL and GMSQ adiabatic NMI was used, whereas diabatic NMI in the GMS domain and adiabatic NMI outside was used in GMSI and GMSH. Following Wergen (1987) the heating rates were held constant during initialization. In all cases, four vertical modes were initialized and four nonlinear iterations were performed. Moisture initialization was not used in these experiments.

The impact of the synthetic moisture data and diabatic heating is considered in terms of precipitation in the model during assimilation and forecast stages, and the spinup. The accumulated precipitation from 14 to 15 January during assimilation and during model forecasts are shown in Figs 6 and 7. (taken from Puri and Davidson, 1992). A marked qualitative improvement is shown with the use of synthetic moisture and heating rates over the CNTL experiment. When compared to the satellite imagery shown in Fig 5, the latter experiment shows little or no precipitation in the region of the tropical cyclone off the west Australian coast and is deficient in the region of the cloud band in the Pacific. A feature of these results is that GMSQ, GMSI and GMSH are more similar to each other than any of them are to CNTL, and that GMSI and GMSH (which use specified heating) are more similar to each other than either is to GMSQ.

An indication of the impact of the GMS-based data on model spinup is given in Fig. 8 (taken from Puri and Davidson, 1992) which shows the 12-h accumulated precipitation accumulated over the domain  $25.7^{\circ}\text{S} - 25.7^{\circ}\text{N}$ ;  $82.5^{\circ}\text{E} - 180^{\circ}\text{E}$  for 5-day model forecasts from 1100 UTC 14 and 15 January. The CNTL forecasts display the typical spinup signature of the model. The GMSQ forecast has similar features but with a reduced amplitude. The GMSI and GMSH forecasts that use GMS-based heating rates in addition to the synthetic moisture have no spinup. Thus for the two cases considered here, the use of information from satellite imagery during data assimilation has the potential to minimize model spin up in the tropics.

Although only precipitation and spin up were considered here, the beneficial impact of the synthetic

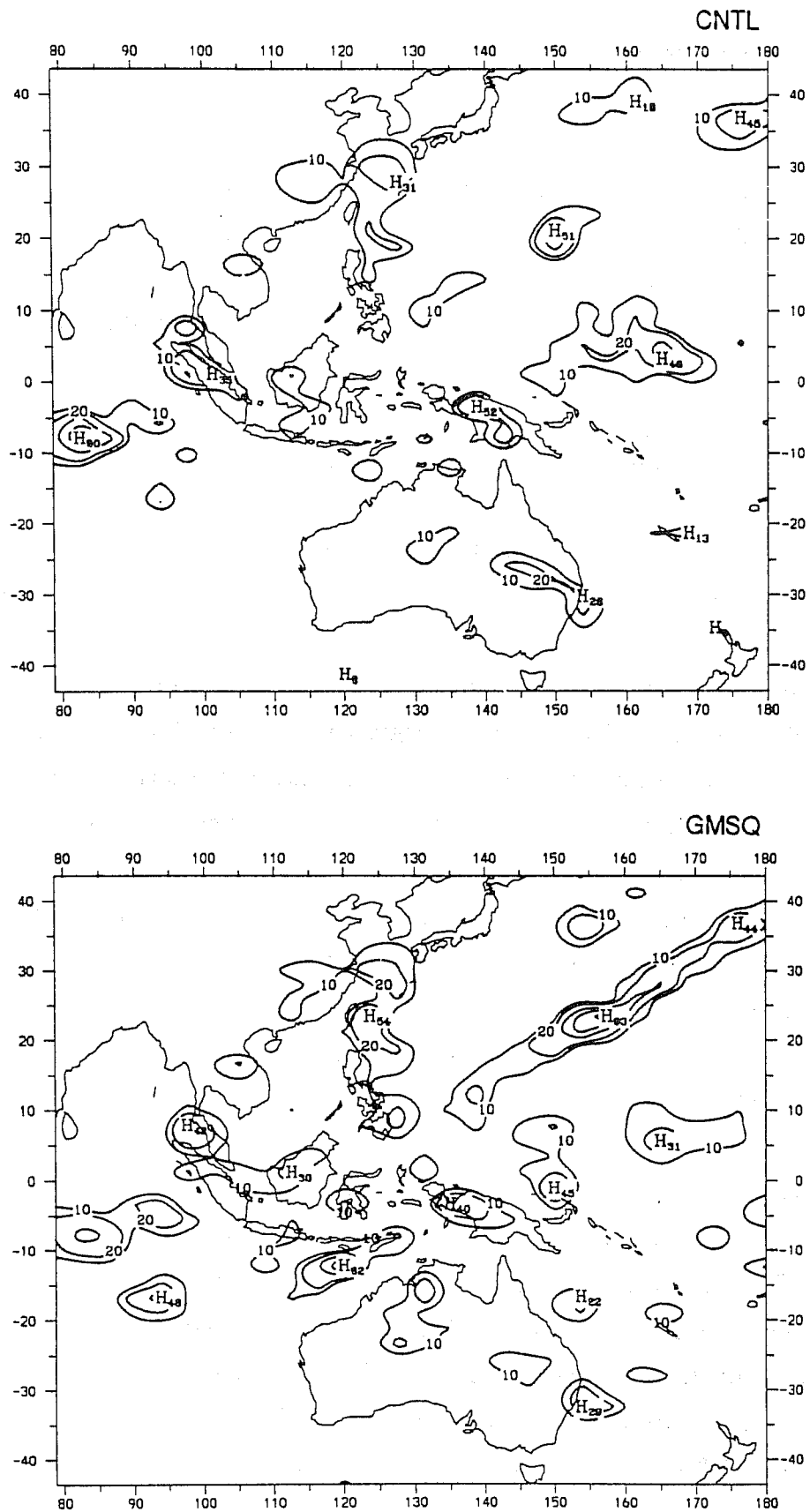


Fig. 6a Accumulated precipitation (mm) during data assimilation from 1100 UTC 14 January 1990 to 1100 UTC 15 January 1990 from CNTL (top) and GMSQ (bottom) experiments. Contours shown are 10, 20, 40, 60, 80 mm day.



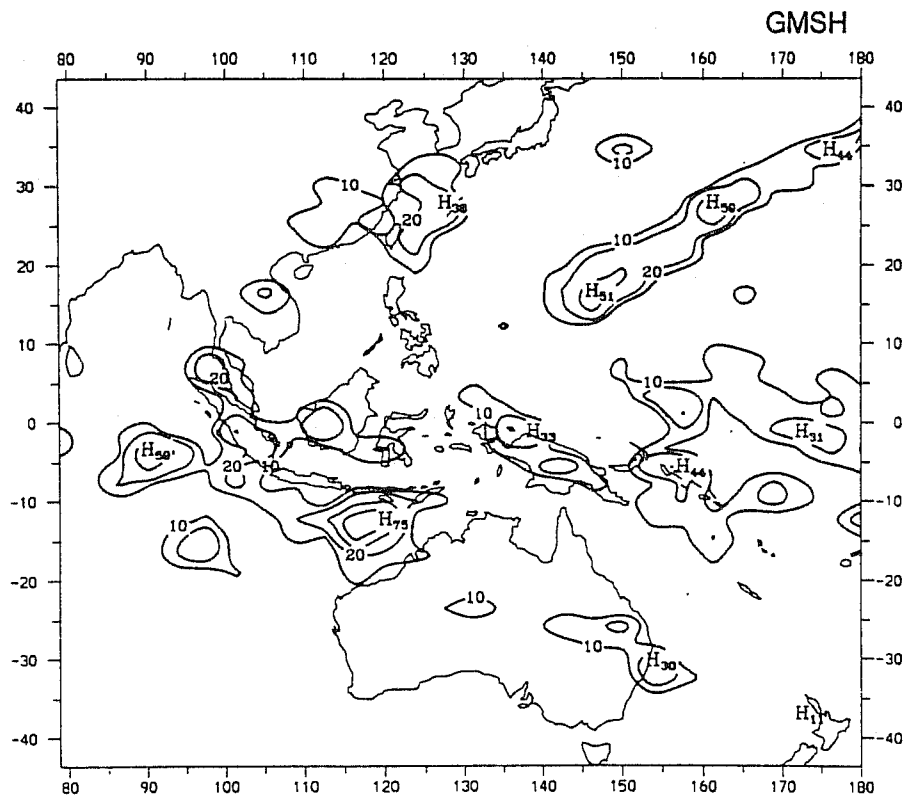
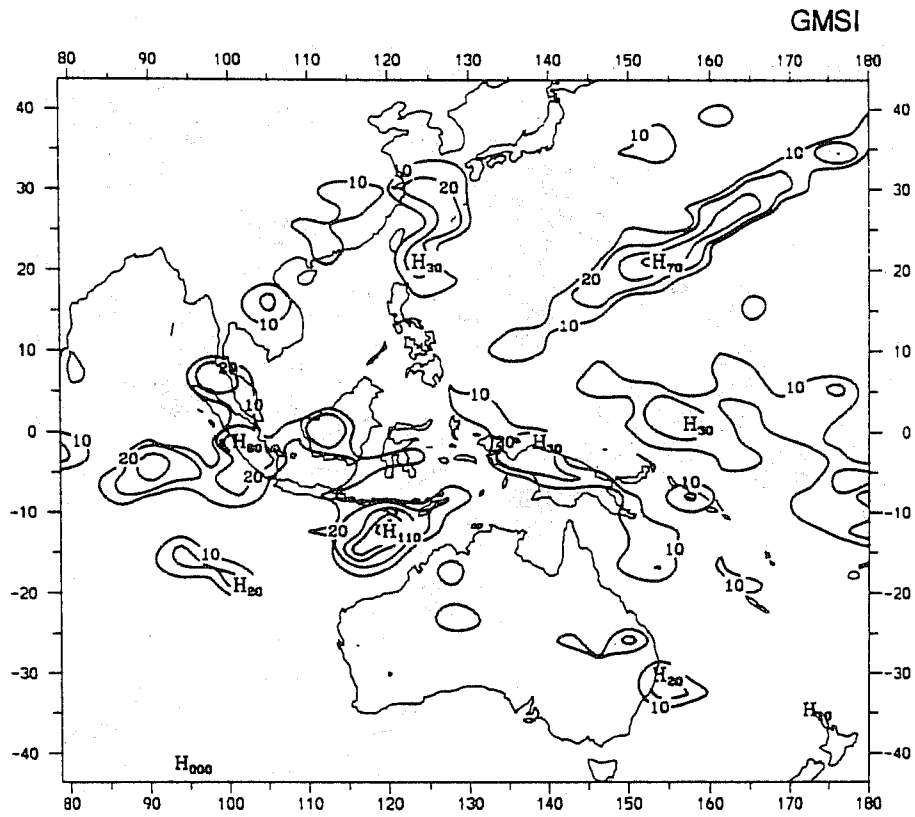


Fig. 6b As in Fig. 6a but for GMSI (top) and GMSH (bottom).

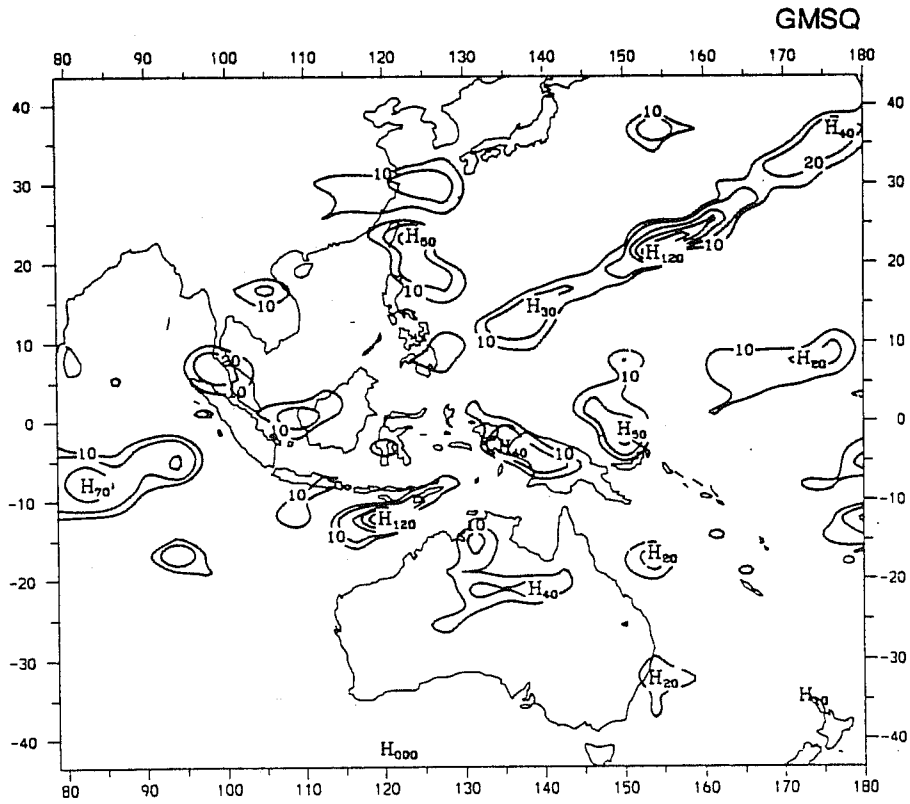
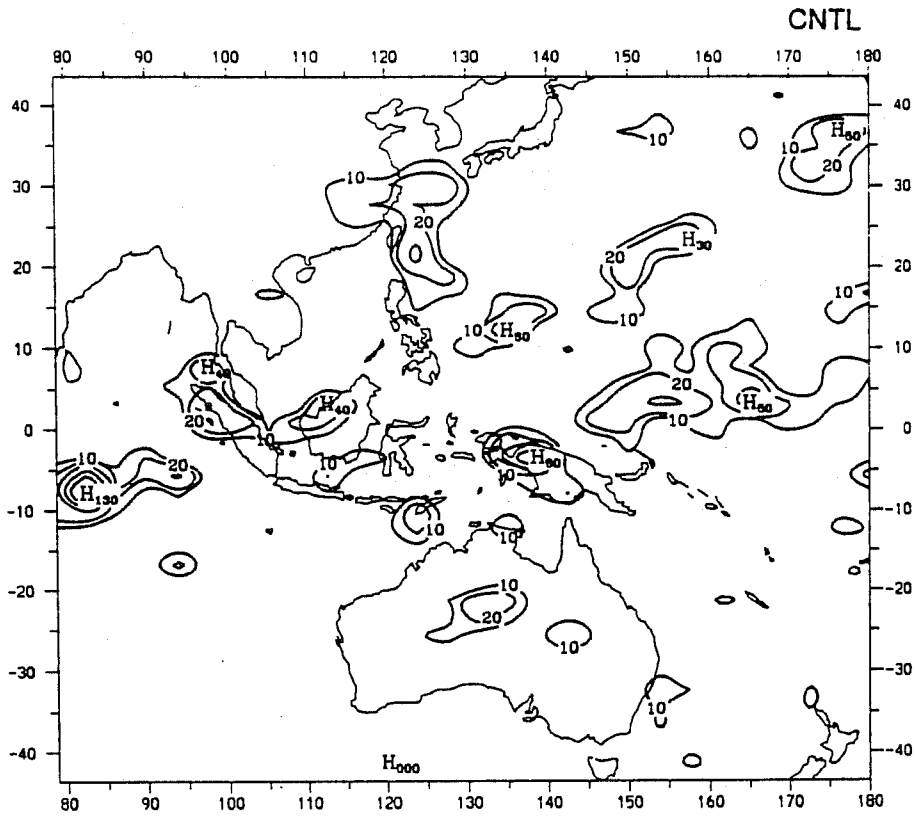


Fig. 7a As in Fig. 6a but for 24-h model forecasts from 1100 UTC 14 January 1990 from CNTL (top) and GMSQ (bottom) analysis.

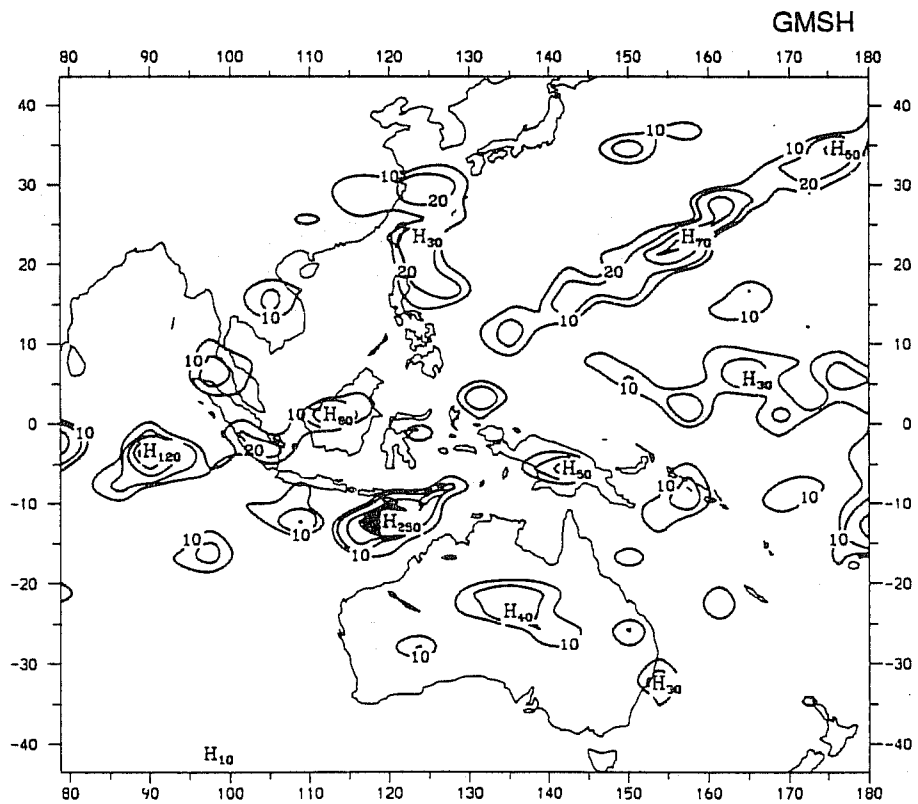
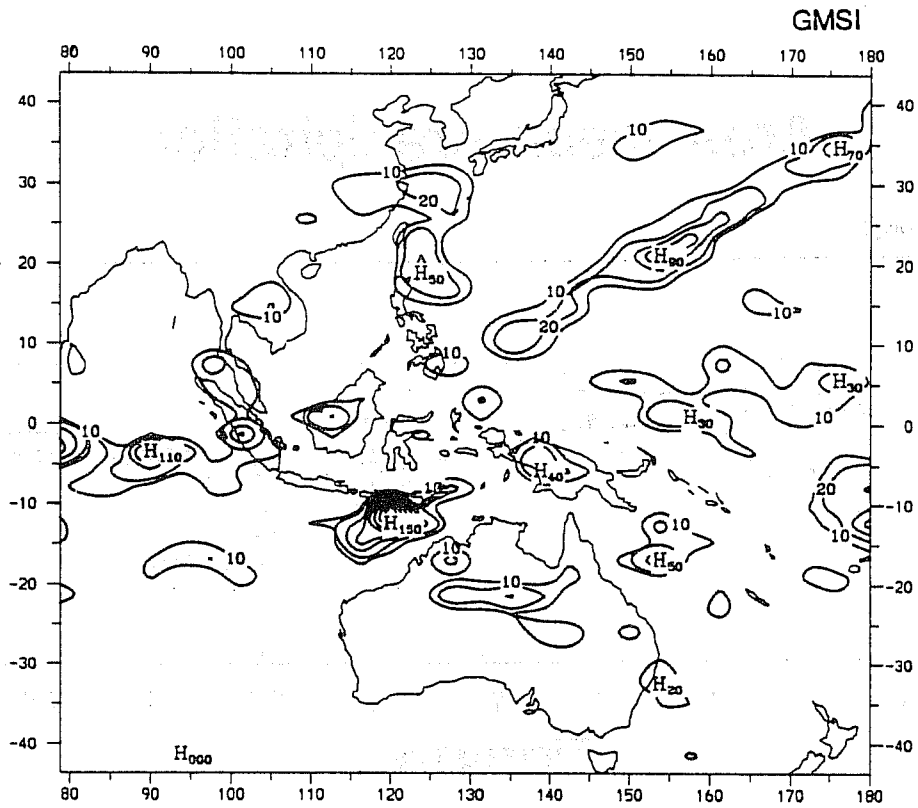
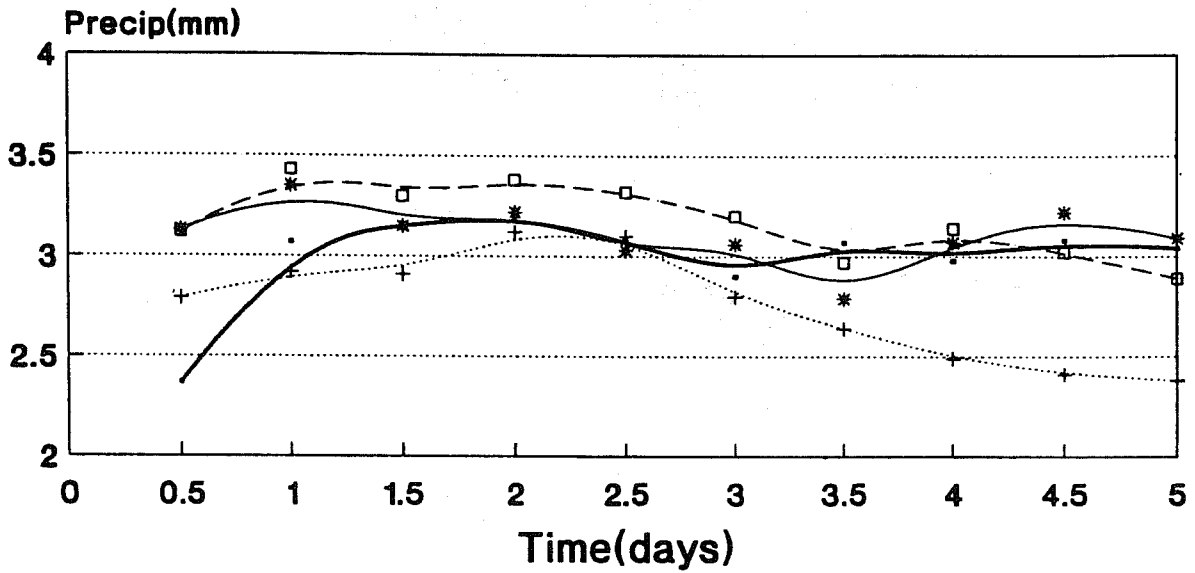
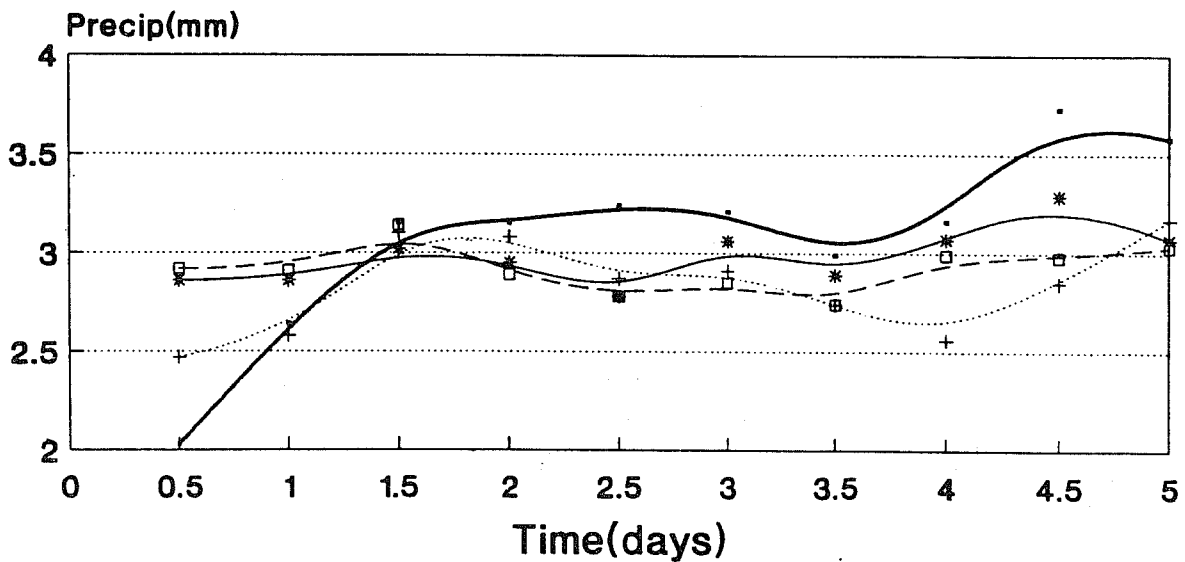


Fig. 7b As in Fig. 7a but for forecasts from GMSI (top) and GMSH (bottom) analyses.

# Area mean precipitation



Forc from Jan 14



Forc from Jan 15

— CNTL    + GMSQ    \* GMSI    -□- GMSH

Fig. 8 Twelve-hour accumulated precipitation (mm) averaged over the domain 25.7°S-25.7°N, 82.5°E-180°E as a function of time for model forecasts from 1100 UTC 14 January 1990 (top) and 1100 UTC 15 January 1990 (bottom) from CNTL, GMSQ, GMSI and GMSH analyses.

moisture data and diabatic heating is not confined to these quantities only. The use of diabatic heating during initialization or early stages of model forecasts also resulted in stronger cyclonic circulation in the region of the cyclones. As with the precipitation, however, these conclusions are only qualitative because of lack of relevant data. Furthermore the results are for a limited number of cases and the conclusions cannot be regarded as definitive. Mills and Davidson (1987), however, also found that the use of synthetic moisture data results in analyses that subjectively better reflect observed cloud features than do analyses that use only conventional data. Further, in some cases, they also found that the additional moisture detail in these analyses can impact positively on model forecasts. As has been indicated above the synthetic moisture data is used operationally at JMA and has been found to have a beneficial impact on moisture analysis and precipitation forecasts (Baba, 1987). Kasahara and Tamiya (1989) have found that the operational JMA global model has little or no spinup and suggest that one of the reasons is the use of GMS cloud data in the moisture analysis.

### 3.2 Impact of moisture initialization

Although the GMSI and GMSH forecasts minimize model spin up in the tropics, examination of the precipitation amount shows significant variation spatially (see Figs. 6b and 7b, for example). One way of overcoming this is to initialize the moisture field as described in section 2.3 so that the precipitation in the early stages of model integration is close to the observed precipitation. Two further data assimilation experiments were performed for the period considered in section 3.1 above namely -

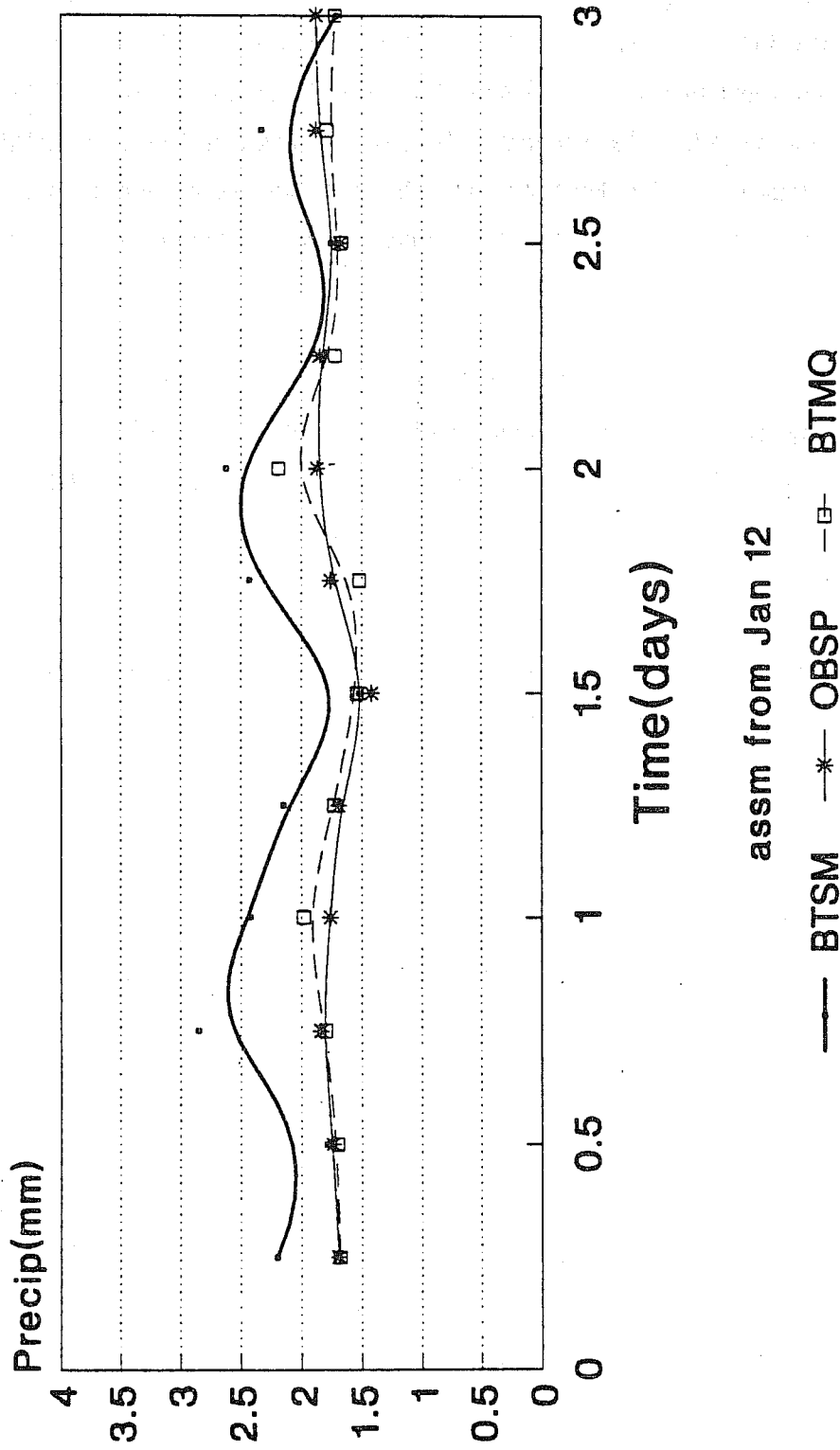
BTSM: As in GMSI experiment but using the Betts-Miller scheme instead of the Kuo scheme,  
and

BTMQ: BTSM + moisture adjustment

Figure 9 (taken from Puri and Davidson, 1992) shows the mixing ratios before moisture adjustment and changes resulting from moisture initialization at 500 hPa in BTMQ for 1100 UTC 14 January. The 500 hPa level is shown because the adjustment scheme is designed to produce maximum changes at this level. The changes in the mixing ratio are small for both cases, with some changes occurring in the cloud band in the Pacific and off the west Australian coast. Fig. 10 (taken from Davidson and Puri, 1992) illustrates the impact of the moisture initialization more graphically. It shows the area mean 6-h accumulated precipitation during data assimilation for the BTSM and BTMQ experiments together with 'observed' precipitation that was used to initialize the moisture field. The precipitation from the BTMQ experiment agrees very closely with the observed precipitation showing the effectiveness of the moisture initialization.



# Area mean precipitation



assm from Jan 12

Fig. 10 Six-hour accumulated precipitation (mm) averaged over the domain 25.7°S-25.7°N, 82.5°E-180°E as a function of time during BTSM and BTMQ assimilation cycles together with the observed precipitation (OBSP).

### 3.3 Impact of synthetic moisture on Australian monsoon onset

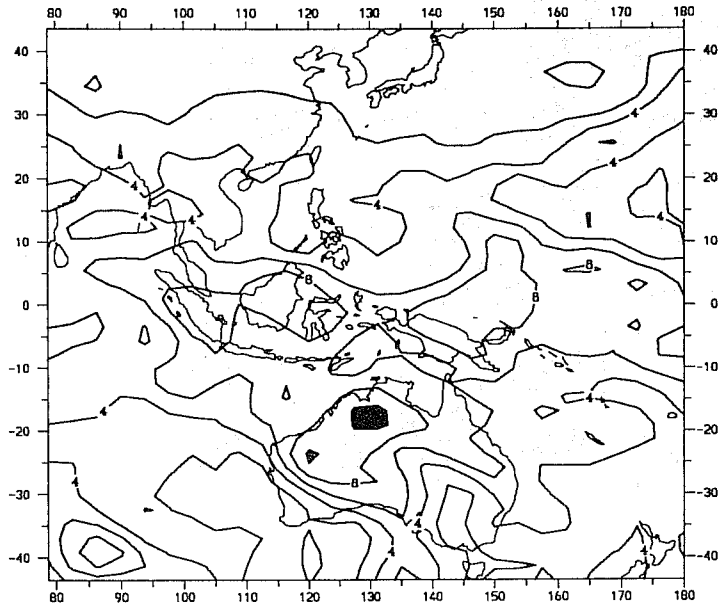
The period considered was the same as phase II of the Australian Monsoon Experiment (AMEX), namely 10 January to 15 February 1987. This period spanned the onset of the Australian summer monsoon which occurred on 14 January as indicated by a number of indices. Following onset there was a weak break from about 14 January to 31 January followed by an active period. Hendon et al. (1989) have carried out a detailed observational analysis on the monsoon data during AMEX and emphasized the important role of low level moisture. The important role of moisture and diabatic heating has also been emphasized by Puri (1994) who has carried a modelling study for the same period.

As was noted above, the analysis of the moisture field in the tropics poses particular problems which are primarily caused by insufficient data. This problem is illustrated in Fig. 11 which shows the 850 hPa moisture analyses for 1200 UTC 10 January 1987 from ECMWF and JMA. The latter analysis which uses moisture data derived from GMS imagery is more moist and shows closer correspondence to the cloud imagery (not shown).

In order to show the impact of the synthetic moisture on monsoon onset model integrations were carried out from 1200 UTC 10 January 1987 from two initial conditions. The first integration used the ECMWF analysis while in the second the JMA mixing ratio only was transplanted into the ECMWF analysis. The starting analysis (MSLP and 850 hPa wind, W850) and the verifying analyses (W850 only) are shown in Figs 12 and 13. Note that in the initial condition the winds over and to the north of northern Australia are weak and show little or no organization. The onset of the monsoon on 14 January can be seen in Fig. 13 which shows the organization and strengthening of the low level westerlies to the north and northwest of Australia. Figs. 14 and 15 show the forecasts from days 2 to 5 from the ECMWF analysis and ECMWF analysis with JMA mixing ratios respectively. The forecast from the ECMWF analysis fails to capture the monsoon onset while the one using JMA mixing ratios generates a well defined monsoon onset and a precipitation pattern (not shown) which shows a broad scale organization over northern Australia evident in the satellite imagery. However the precipitation and onset occur about two days early. This could be due to the JMA analysis being too moist. Moreover the use of an analysis generated by a data assimilation system in which the model used is different from the BMRC model could lead to spin up in both integrations. Both these problems could be reduced through moisture initialization and the use of diabatic NMI using specified heating rates described earlier. The successful prediction of onset with JMA mixing ratios also has impact on a longer term integration extending out to 15 February. Although not shown here, this



ECMWF ANALYSIS FOR 1200UTC JAN 10 1987



JMA ANALYSIS FOR 1200UTC JAN 10 1987

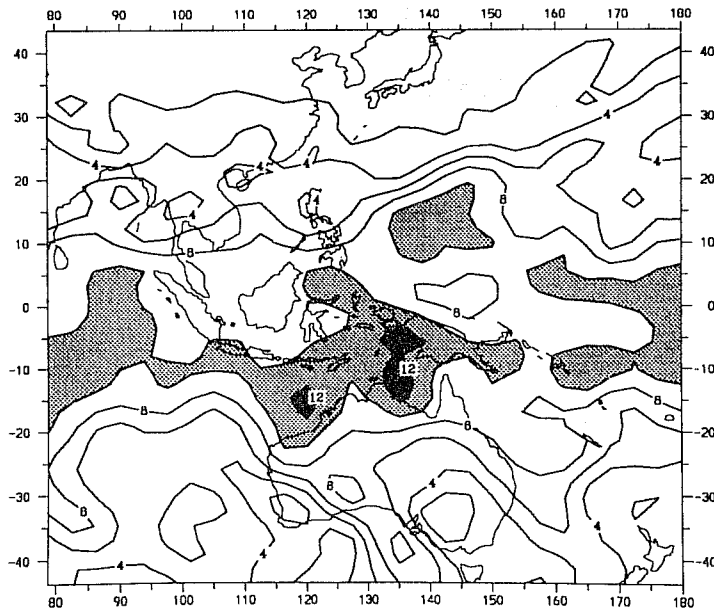
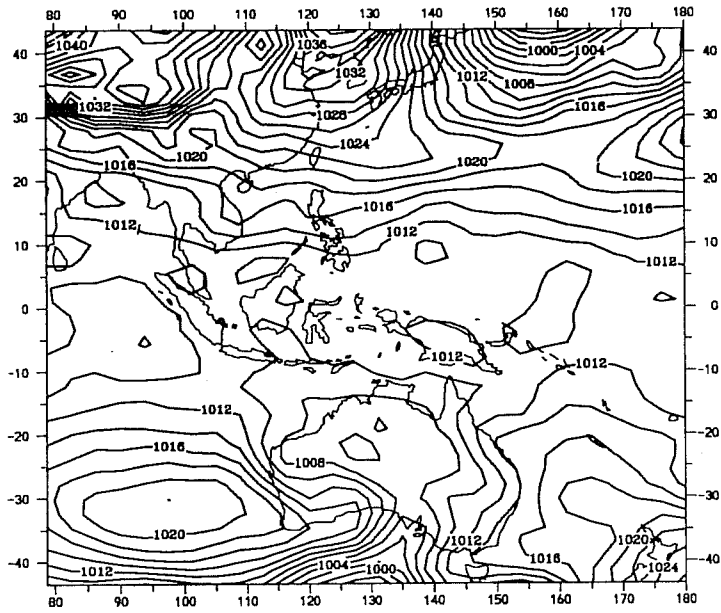


Fig. 11 Mixing ratio ( $\text{g kg}^{-1}$ ) at 850 hPa for 1200 UTC 10 January 1987 ECMWF (top) and JMA (bottom) analyses. Contour interval is  $2 \text{ g kg}^{-1}$  and values greater than  $10 \text{ g kg}^{-1}$  are shaded.

ECMWF ANALYSIS FOR 1200 UTC JAN 10 1987



ECMWF ANALYSIS FOR 1200 UTC JAN 10 1987

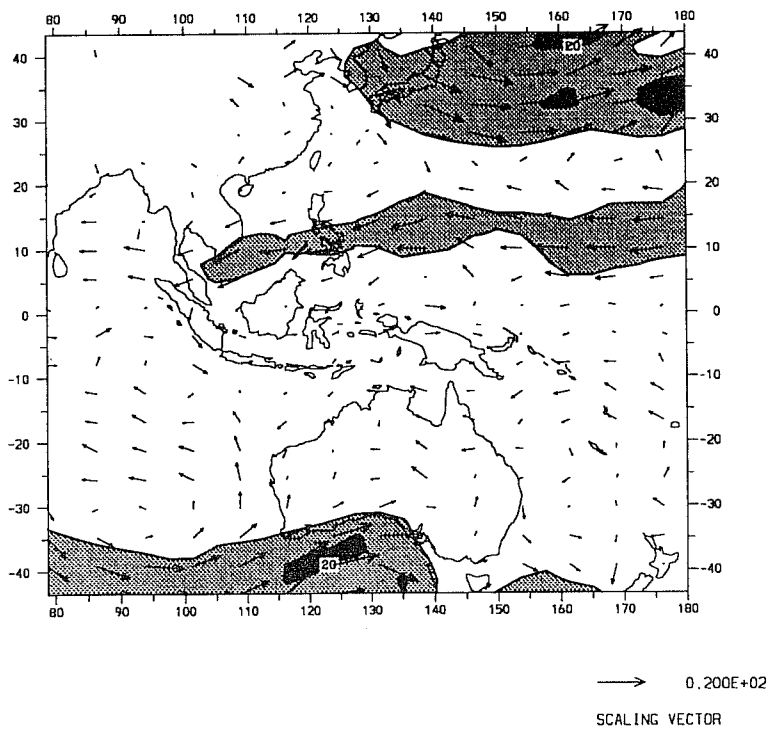
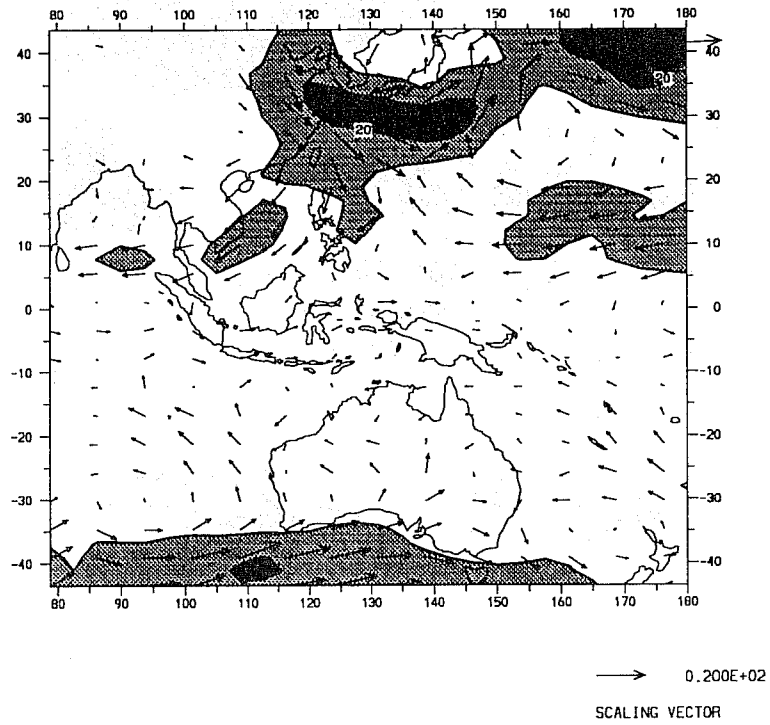


Fig. 12 ECMWF analyses for MSLP (hPa, top) and W850 ( $\text{ms}^{-1}$ , bottom) for 1200 UTC 10 January 1987. Contour intervals are 2hPa and  $10\text{ms}^{-1}$  and wind magnitudes greater than  $10\text{ms}^{-1}$  are shaded.

ECMWF ANALYSIS FOR 1200UTC JAN 12 1987



ECMWF ANALYSIS FOR 1200UTC JAN 13 1987

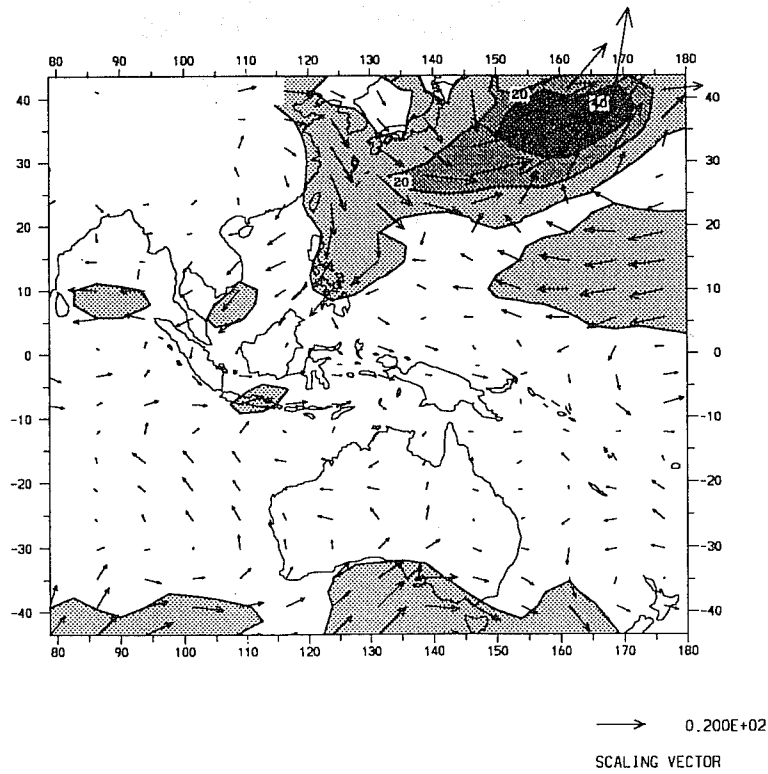
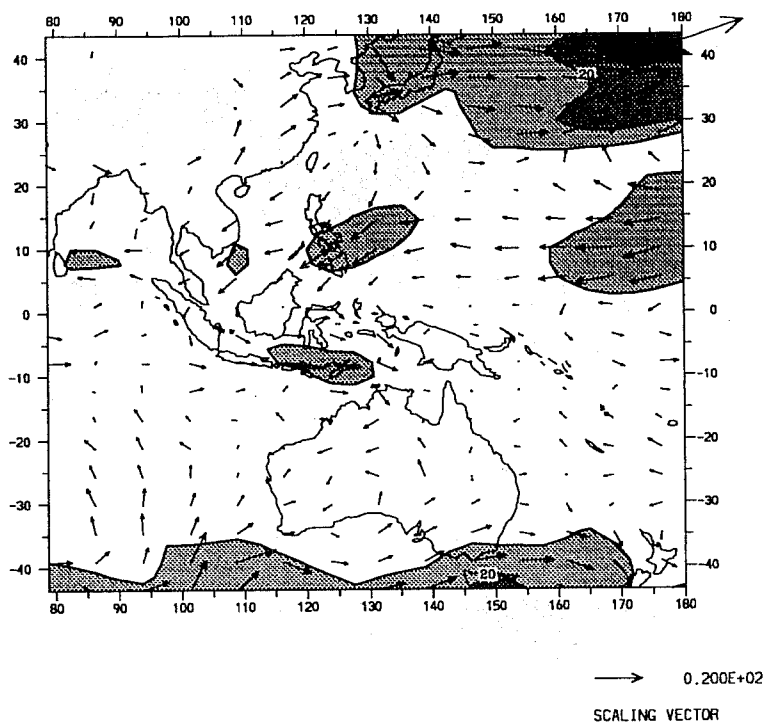


Fig. 13a ECMWF analyses for W850 ( $\text{ms}^{-1}$ ) for 1200 UTC 12 January (top) and 13 January 1987 (bottom). Contour interval for isotachs is  $10 \text{ ms}^{-1}$  and values greater than  $10 \text{ ms}^{-1}$  are shaded.

ECMWF ANALYSIS FOR 1200UTC JAN 14 1987



ECMWF ANALYSIS FOR 1200UTC JAN 15 1987

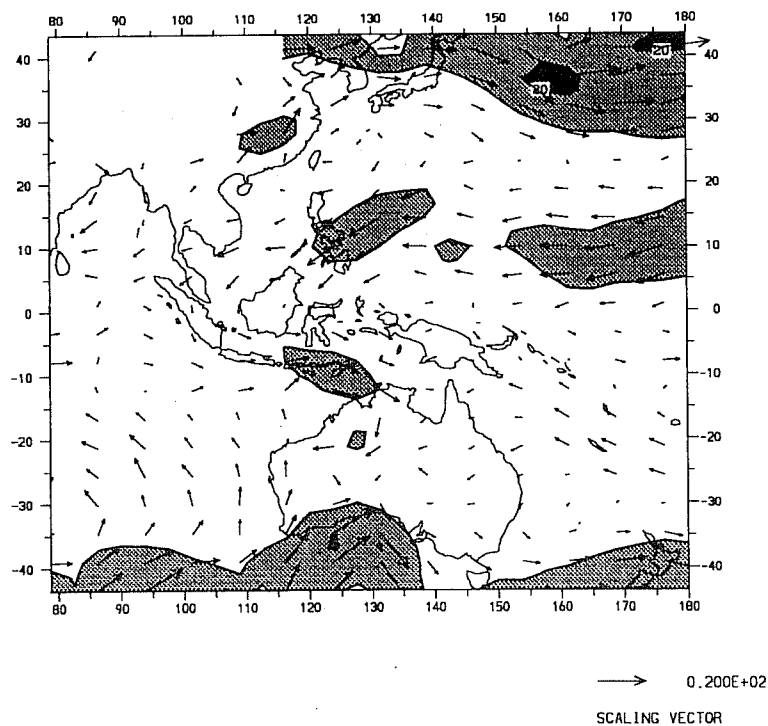
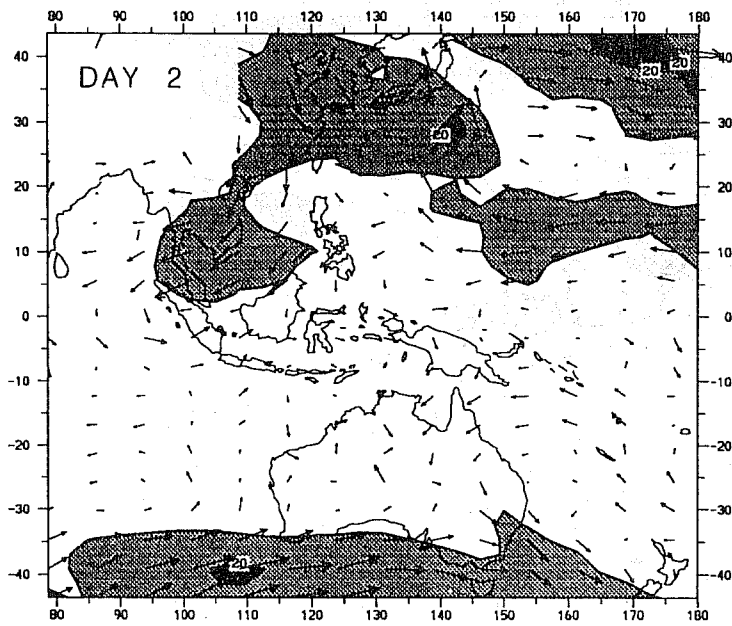


Fig. 13b As in Fig. 13a but for 1200 UTC 14 January (top) and 15 January 1987 (bottom).

FORECAST FROM 1200 UTC 10 JAN 1987 ECMWF IC



FORECAST FROM 1200 UTC 10 JAN 1987 ECMWF IC

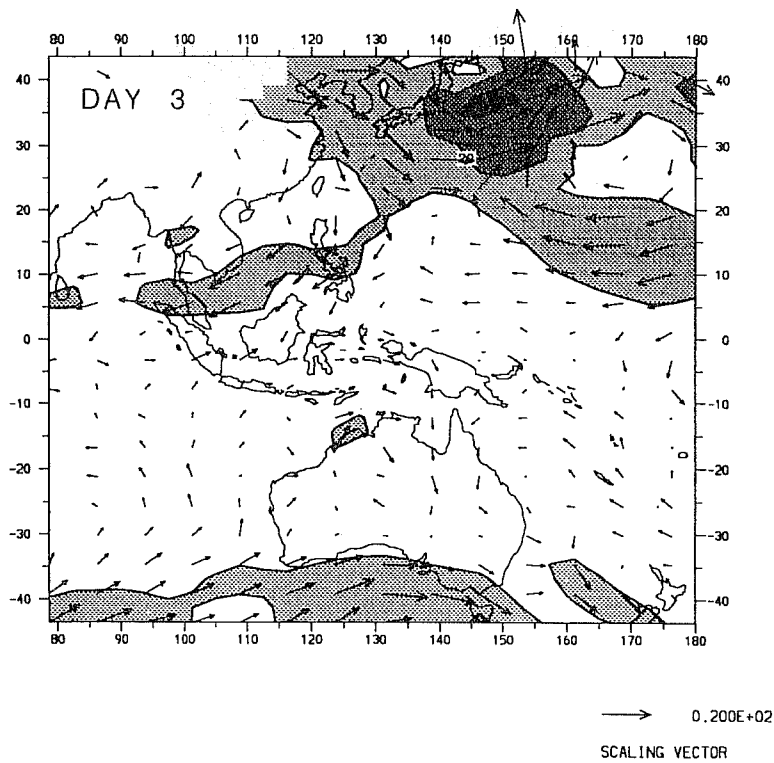
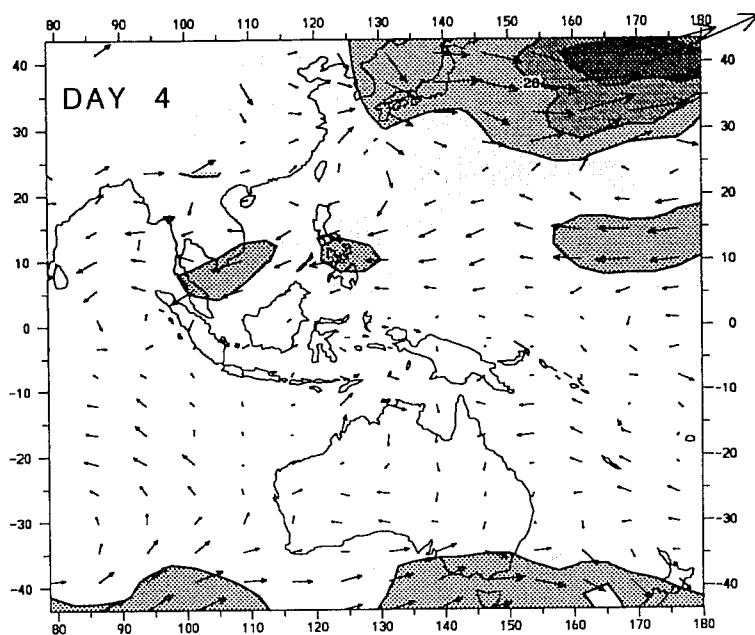
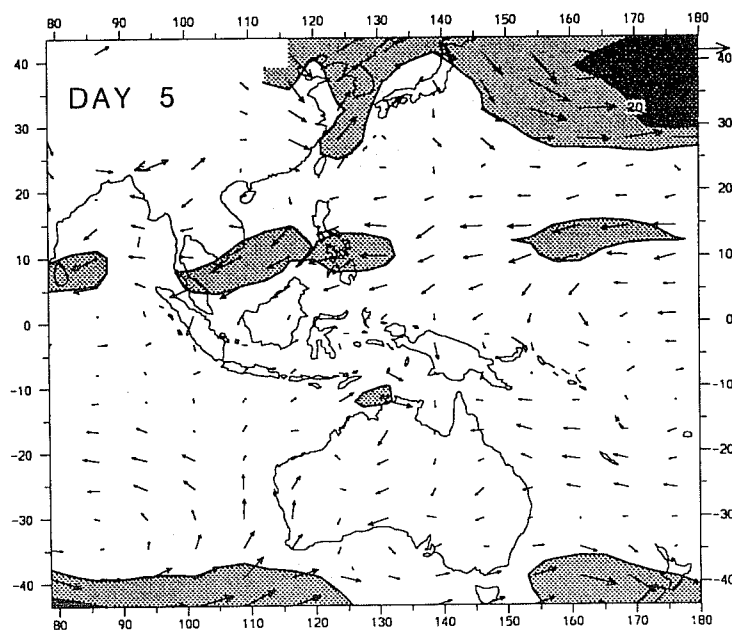


Fig. 14a Forecasts for W850 for day 2 (top) and day 3 (bottom) starting from 1200 UTC 10 January 1987 ECMWF analysis. Contour intervals for isotachs is  $10\text{ms}^{-1}$  and values greater than  $10\text{ms}^{-1}$  are shaded.

FORECAST FROM 1200 UTC 10 JAN 1987 ECMWF IC



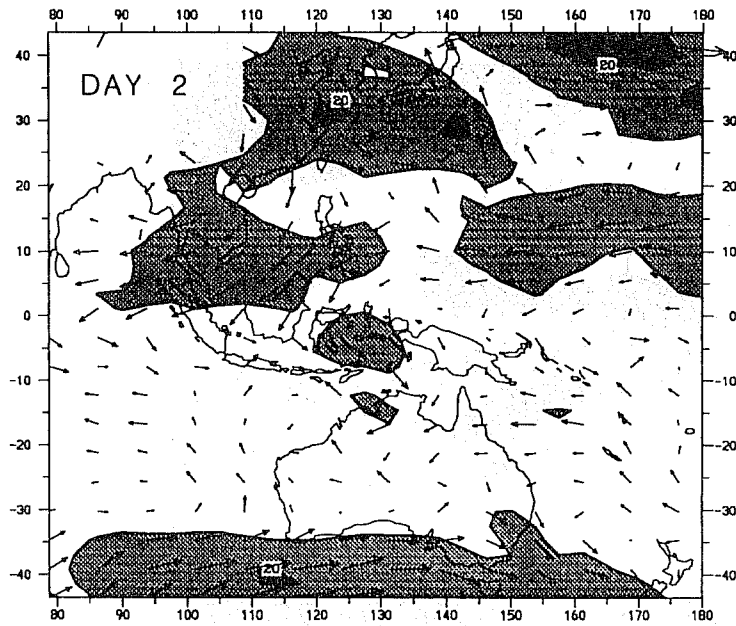
FORECAST FROM 1200 UTC 10 JAN 1987 ECMWF IC



→ 0.200E+02  
SCALING VECTOR

Fig. 14b As in Fig. 14a but for day 4 (top) and day 5 (bottom).

FORECAST FROM 1200 UTC 10 JAN 1987 JMA MIXR



FORECAST FROM 1200 UTC 10 JAN 1987 JMA MIXR

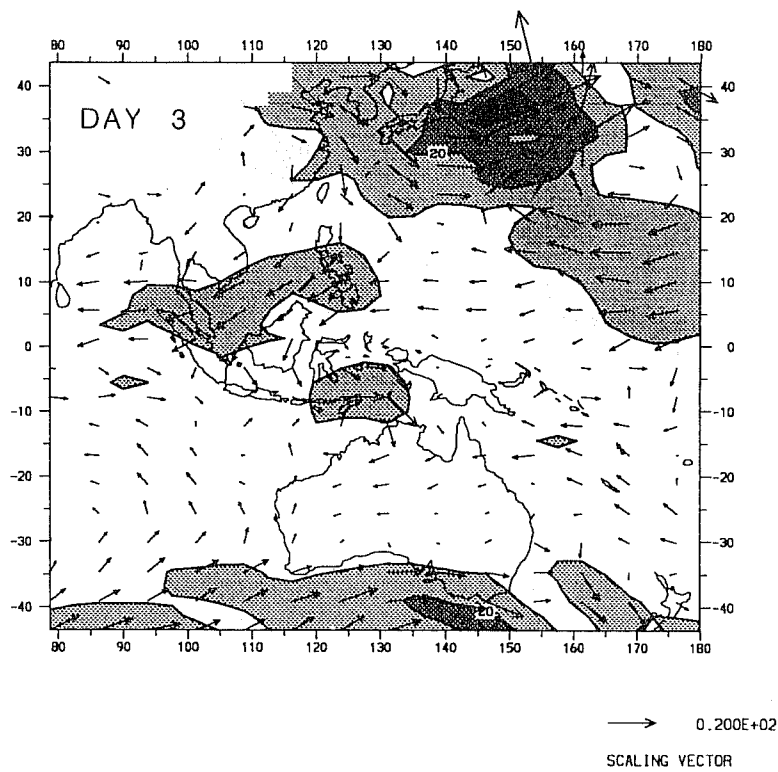
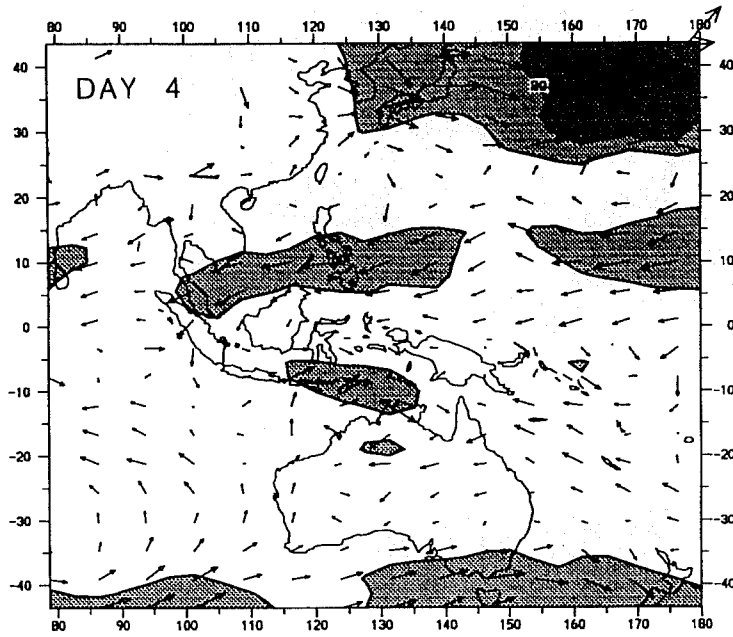
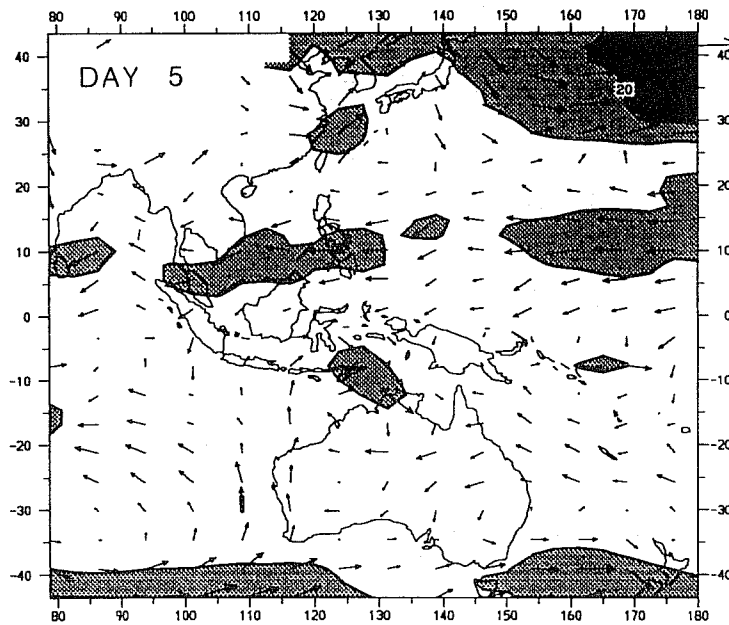


Fig. 15a As in Fig. 14a but for forecasts from ECMWF analysis transplanted with JMA mixing ratios.

FORECAST FROM 1200 UTC 10 JAN 1987 JMA MIXR



FORECAST FROM 1200 UTC 10 JAN 1987 JMA MIXR



→ 0.200E+02  
SCALING VECTOR

Fig. 15b As in Fig. 15a but for day 4 (top) and day 5 (bottom).



integration simulates most of the features of the monsoon during the AMEX period including onset and the active and break periods (Puri, 1994).

It should be noted that similar experiments on the Australian monsoon onset have been performed at JMA by Kuma (1993) which show that the use of satellite based moisture data results in successful prediction of onset by the JMA global spectral model, again emphasizing the important role of the moisture analysis.

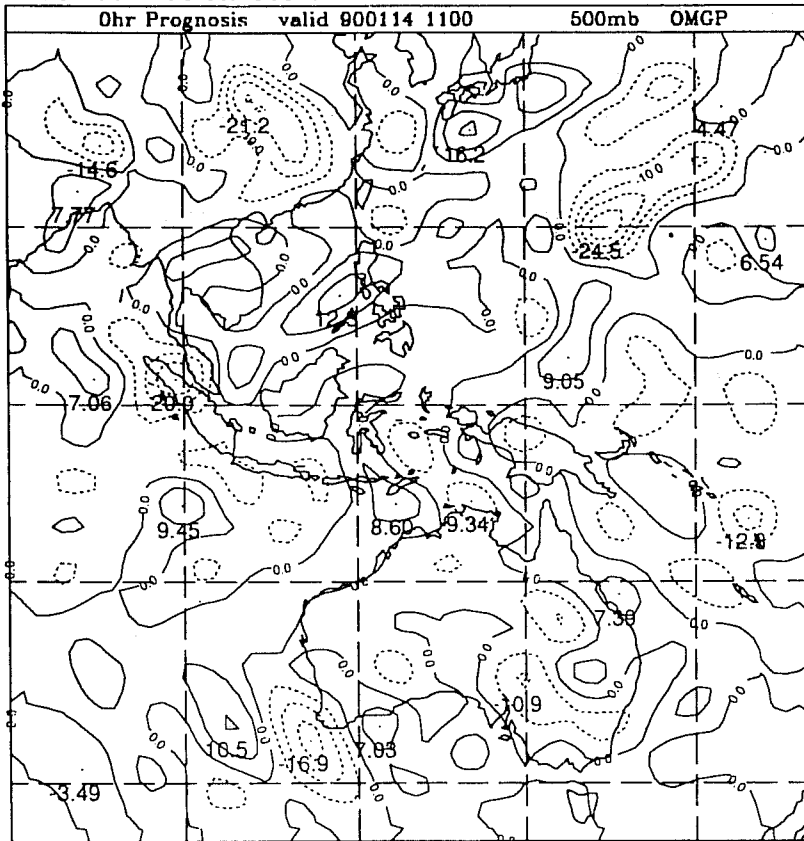
#### 4. PRACTICAL APPLICATIONS

##### 4.1 Operational application in TAPS

TAPS has been running operationally since November 1992 at a horizontal resolution of 95 km and 19 sigma levels. Two day forecasts are performed twice daily from 0000 UTC and 1200 UTC. The system makes extensive use of GMS based data namely moisture, heating and tropical cyclone bogus data. The moisture data and cloud top temperatures are extracted four times a day and bogus tropical cyclone data are included whenever a named cyclone is in the domain.

As was noted earlier, the heating rate information is incorporated into TAPS through the use of diabatic dynamical nudging during which the heating rates from the Kuo parameterization used in TAPS are replaced by satellite derived heating rates. Although longer nudging periods are desirable (at least 24 hours), operational constraints only allow 12 hours of nudging. One of the perceived benefits of nudging is that it should define a more realistic vertical motion through the use of observationally based heating distributions. An example of this is shown in Fig. 16 (taken from Davidson and Puri, 1992) which shows the 500 hPa vertical motion field after diabatic vertical mode initialization of the target analysis (following Bourke and McGregor, 1983) and after 24 hours of dynamical nudging and satellite-defined heating. Features to be particularly noted are the close correspondence between the satellite imagery (Fig 5a) and the vertical motion field from the diabatic nudging particularly for the three cyclones and the major convective areas, and the general lack of coherence between the imagery and the vertical motion after diabatic initialization. Detailed evaluation of nudging (Davidson and Puri, 1992) indicates that this form of tropical diabatic initialization has the potential to define vertical motions consistent with satellite cloud imagery and improve mass wind balance in the initial conditions. Davidson et al. (1993) have studied the impact of nudging on the retention of tropical cyclone circulations in TAPS. They showed that the method of assimilation and initialization of the bogussed vortex can have a large effect on the imposed

Vertical motion after initialization



Vertical motion after 24 hrs of dynamic nudging

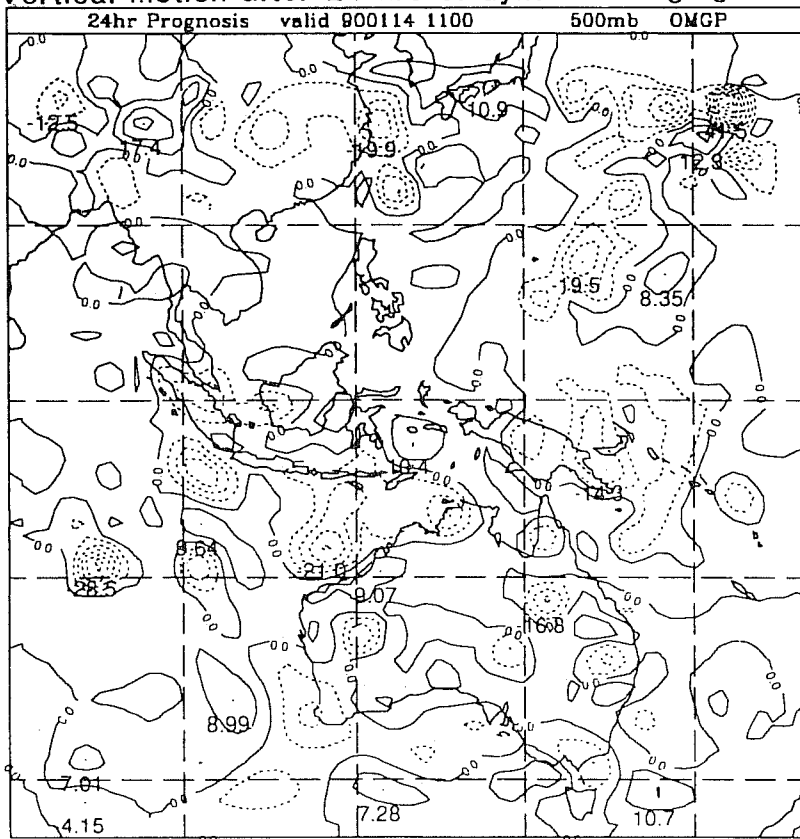


Fig. 16 500 hPa vertical motion field ( $\text{hPa h}^{-1}$ ) after initialization of target analysis (top), and after 24h of dynamical nudging and satellite-defined heating (bottom).

structure and can affect the quality of prediction of both the cyclone itself and the large scale flows quite remote from the storm centre. Inadequate forms of processing can result in either a complete rejection of the imposed vortex, or mass wind adjustments beyond the scale of the cyclone's circulation. The method of diabatic nudging used in TAPS is effective in reducing the impact of these problems.

The use of synthetic moisture in conjunction with GMS based heating rates and dynamical nudging has had a positive impact in delineating clouds in the initial state and precipitation prediction. Fig.17 shows the total cloud distribution in the initial condition after 12 hours of nudging valid for 1100 UTC 30 January and 31 January 1994. Comparison with the imagery shown in Fig. 18 shows a good correspondence. This is perhaps not surprising since the diagnostic cloud scheme in the model is based on relative humidity which was analysed using GMS imagery. However there is a significant improvement over the GASP analysis (not shown) which does not use synthetic moisture and which provides the first guess for TAPS. Some of the improvement in the initial cloud specification carries over to the one day forecast also shown in Fig. 17. Although there are deficiencies, the forecast cloud cover shows reasonable agreement with the imagery shown in Fig 18.

TAPS has shown some skill in predicting heavy rainfall events. The period considered above included a heavy rainfall event around Cairns in north east Australia. This can be clearly seen in the cloud imagery and rainfall analyses based on rainguage data only (see Fig. 22) which shows heavy rainfall in the region around Cairns. The one and two day precipitation predictions from 1100 UTC 29 January from TAPS are shown in Fig 19. Although the maximum amounts are underestimated, the model prediction shows considerable skill in predicting this event.

Mathur et al. (1992) have used a nudging procedure in conjunction with satellite derived rainfall in the National Meteorological Center (Washington) medium range forecast model (MRF). In their experiments, which included data assimilation, the convective parameterization was modified to adjust the predicted rainfall amounts towards observations. Their results, based on a number of case studies, show an improvement in intensity and location of the intertropical convergence zone and tropical disturbances with the application of the nudging procedure. Additionally, spurious cyclones and excessive rainfall that were predicted without this procedure either failed to form or their intensities were considerably reduced. The use of a modified convective scheme (or physical initialization) in the global data assimilation resulted in an improvement in the rainfall amounts. Mathur et al. also emphasized the need for more accurate and greater coverage of observations of rainfall over short time periods for optimal use of such data.

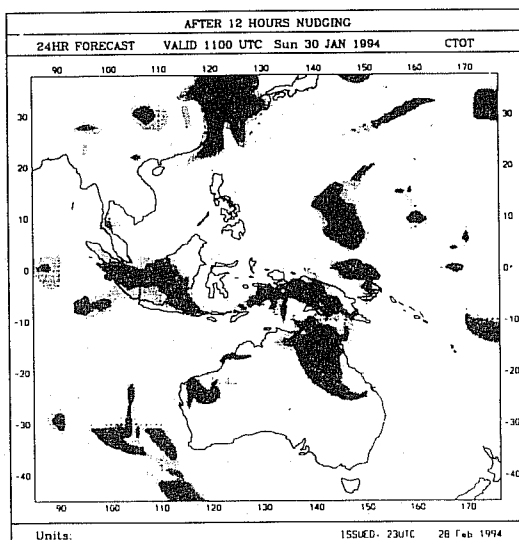
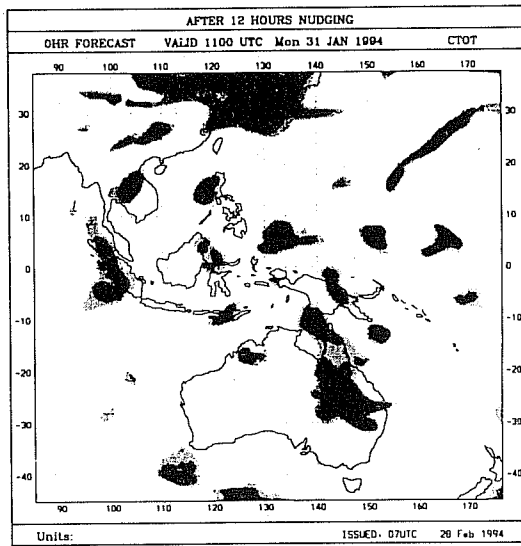
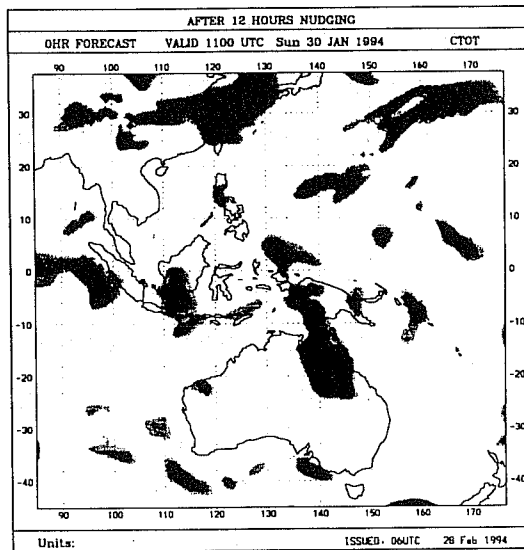


Fig. 17 Total cloud distribution after 12-h nudging for 1100 UTC 30 January 1994 (top), 31 January (middle), and 24-h forecast from 29 January (bottom).

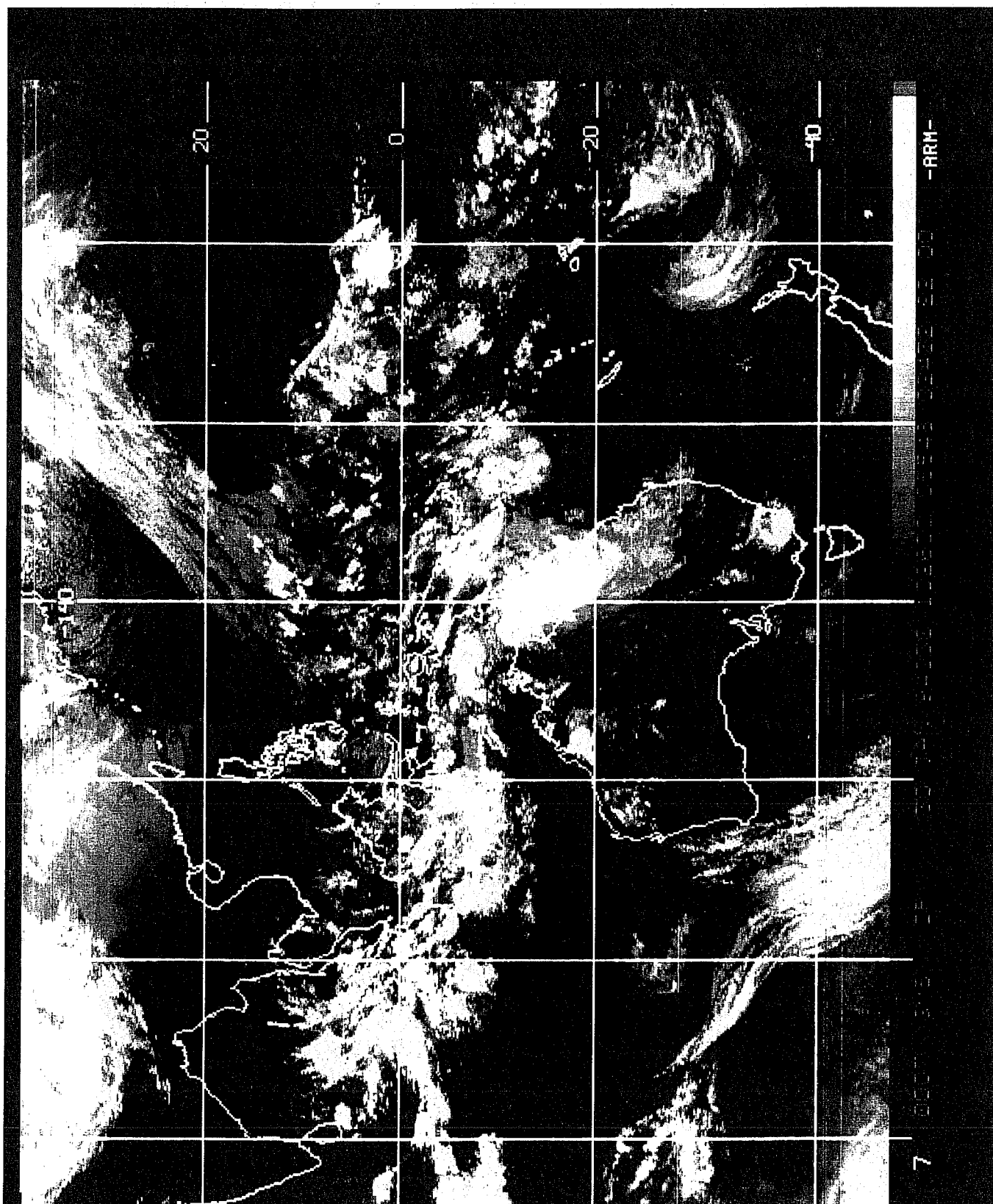


Fig. 18a GMS infrared imagery for 1100 UTC 30 January 1994.

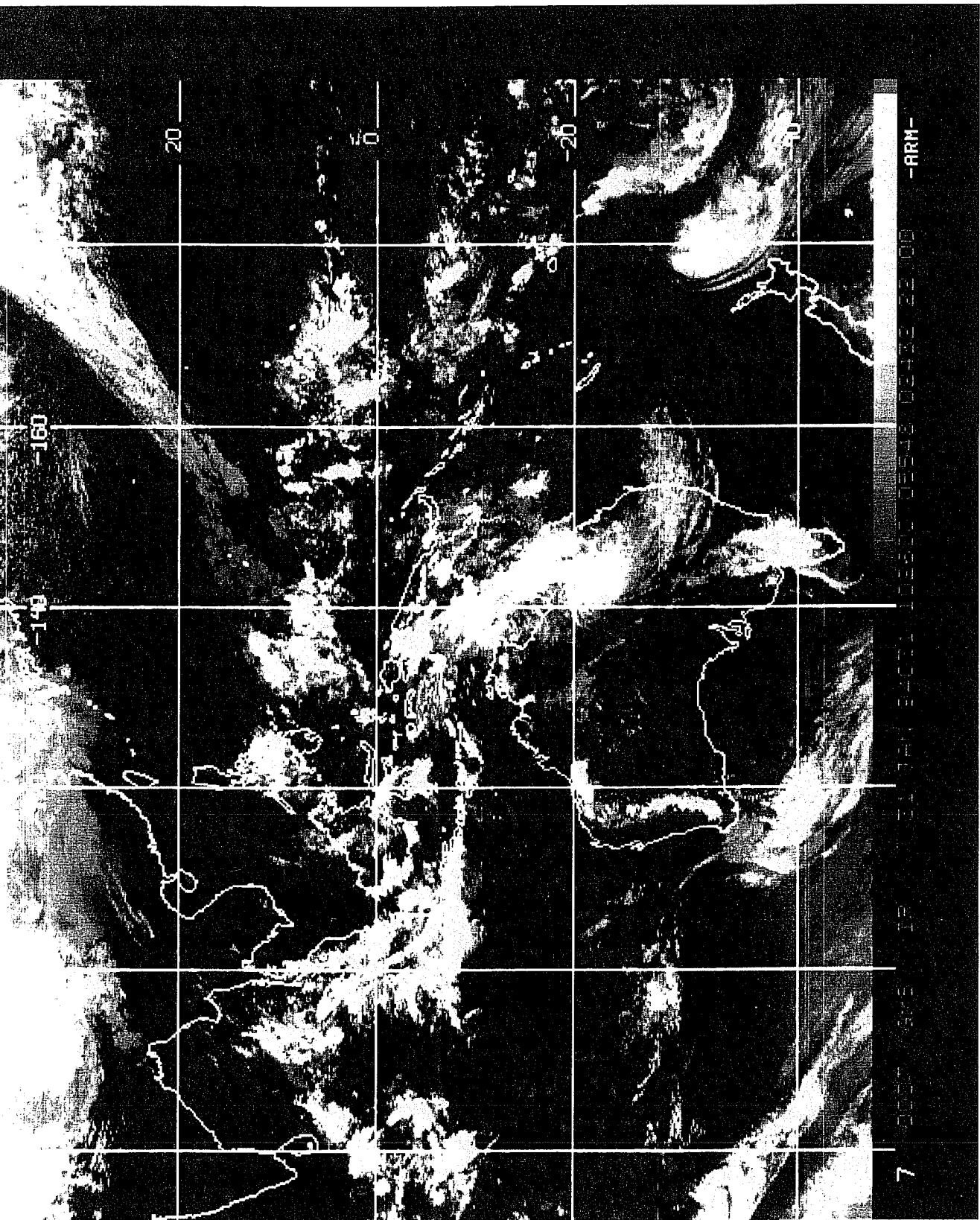


Fig. 18b As in Fig. 18a but for 1100 UTC 31 January 1994.

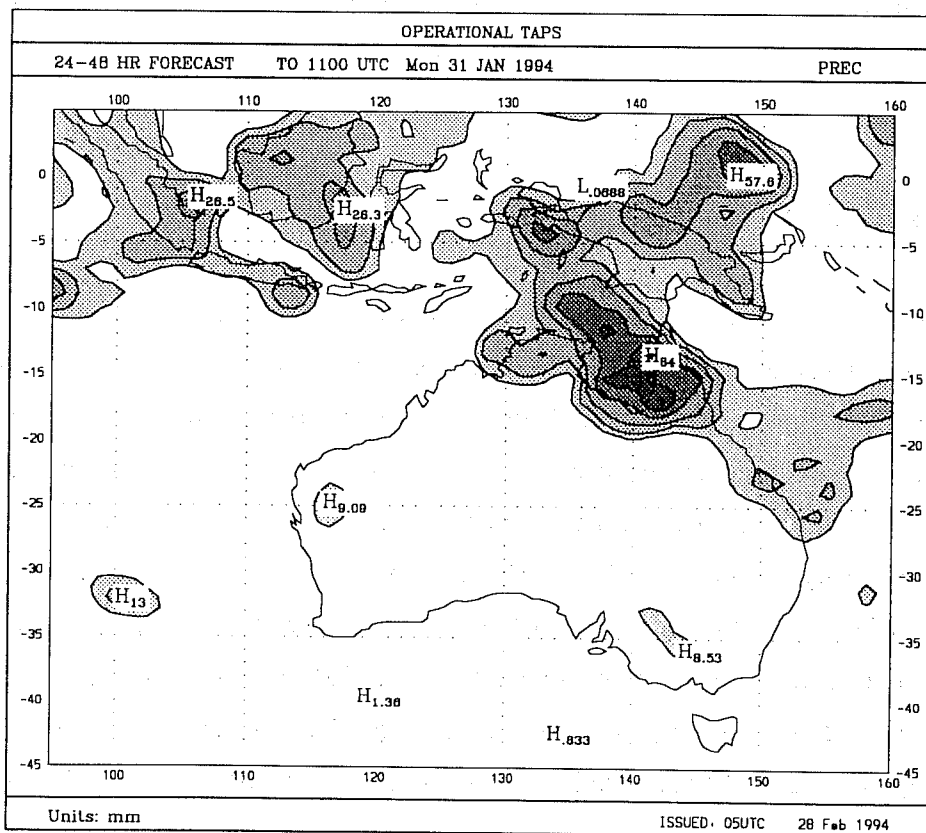
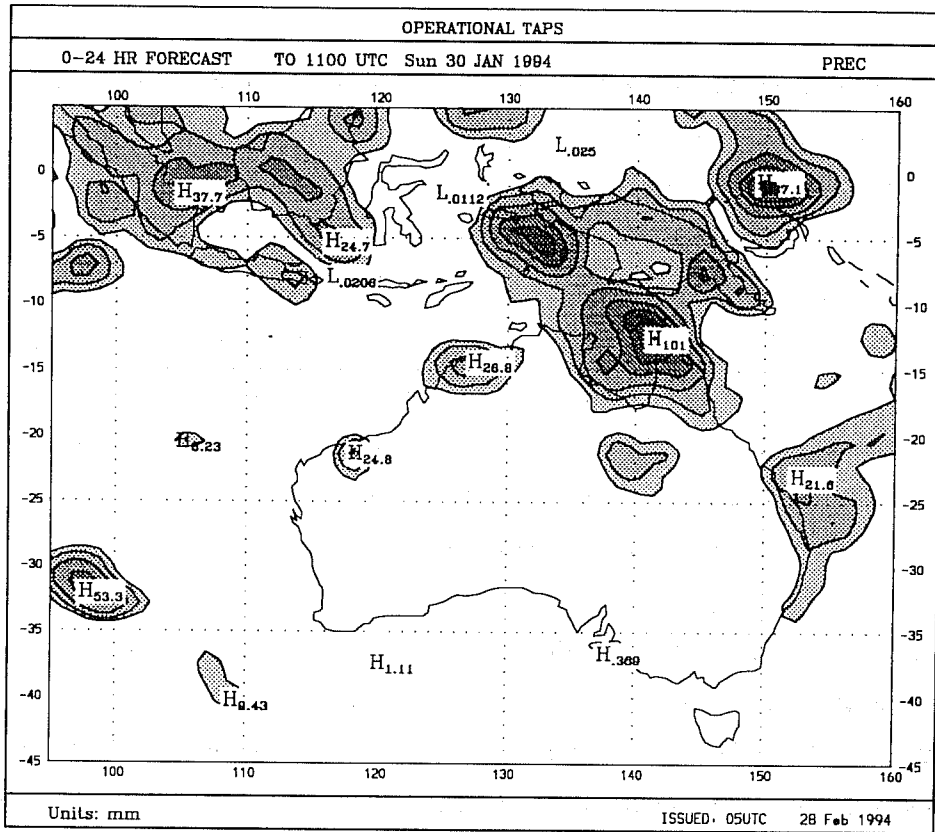


Fig. 19 1 and 2 day rainfall predictions from TAPS from 1100 UTC 29 January 1994.

## 4.2 Related developments in operational systems

As was noted earlier the moisture analysis in GASP uses a Cressman type algorithm whereas a univariate optimum interpolation scheme is used in TAPS with the synthetic moisture assigned the same weights as sondes. However, given the important role played by moisture in the tropics, the moisture analysis for both systems is being improved. The new analysis scheme will use statistical interpolation and the design of the analysis scheme closely follows the multivariate statistical interpolation formulation used for the other fields. The new moisture analysis scheme will provide greater flexibility in terms of assigning different weights to observation platforms and will also allow precipitable water data to be used for moisture analysis. The horizontal and vertical correlations and observational errors closely follow the ECMWF specifications. Data assimilation experiments to validate the new scheme have already been carried out.

Work has commenced in implementing the synthetic moisture data in GASP using the improved moisture analysis scheme described above. Preliminary data assimilation experiments have been performed and Figs 20(a) and (b) show the mixing ratio analyses at 850 hPa and 700 hPa from operational GASP using conventional moisture data and after 10 days of data assimilation using conventional + synthetic moisture data in the new scheme respectively. Although the patterns are broadly similar, the analysis using the synthetic moisture shows narrower tongues of moist zones compared to the conventional data only case. The former analysis is in better qualitative agreement to the TAPS analysis (Fig 20c) and the imagery shown in Fig. 21.

## 5. FUTURE WORK

The procedures for obtaining heating rates and moisture initialization rely on obtaining reasonable estimates of observed precipitation. The estimates of rainfall from satellites currently have large errors. However considerable effort is being devoted towards improving daily satellite-derived precipitation rates and a number of intercomparisons between various schemes in regions of good ground based observational data base have been performed under the auspices of the Global Precipitation Climatology Program (GPCP). The SSM/I instrument also has the potential to provide improved estimates of precipitation when these data becomes available in real time. A number of algorithms have been derived for estimating rainfall from the SSM/I sensor (See Olson et al, 1990 and Kummerow and Giglio (1993), for example) and algorithm intercomparison exercises are currently under way. Ultimately though rainfall analysis will have to be based on a mix of conventional rainfall observations with satellite estimates, possibly using numerical model estimates as a first guess.



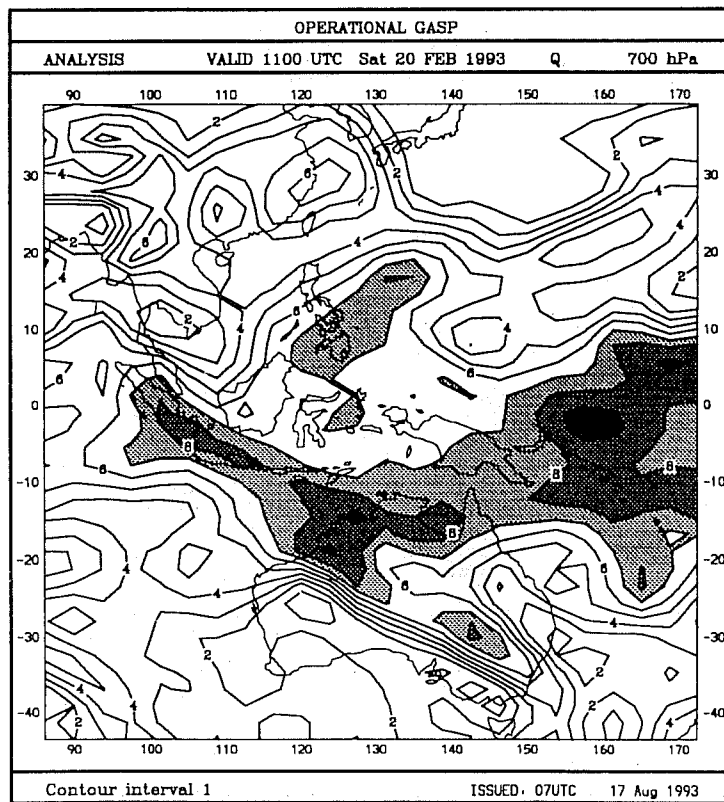
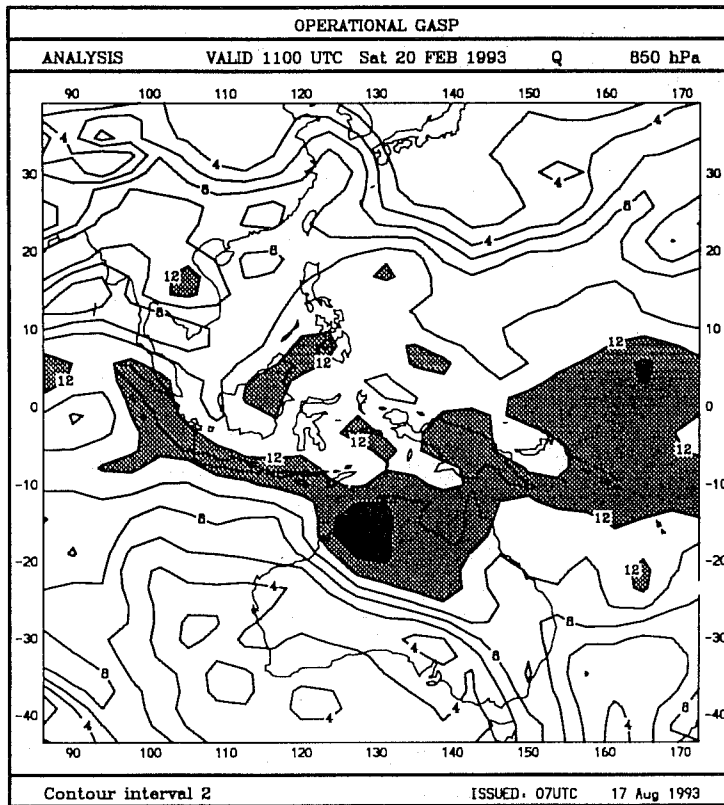


Fig. 20a Mixing ratio analyses at 850 hPa (top) and 700 hPa(bottom) for 1100 UTC 20 February 1993 using conventional moisture data only in GASP.

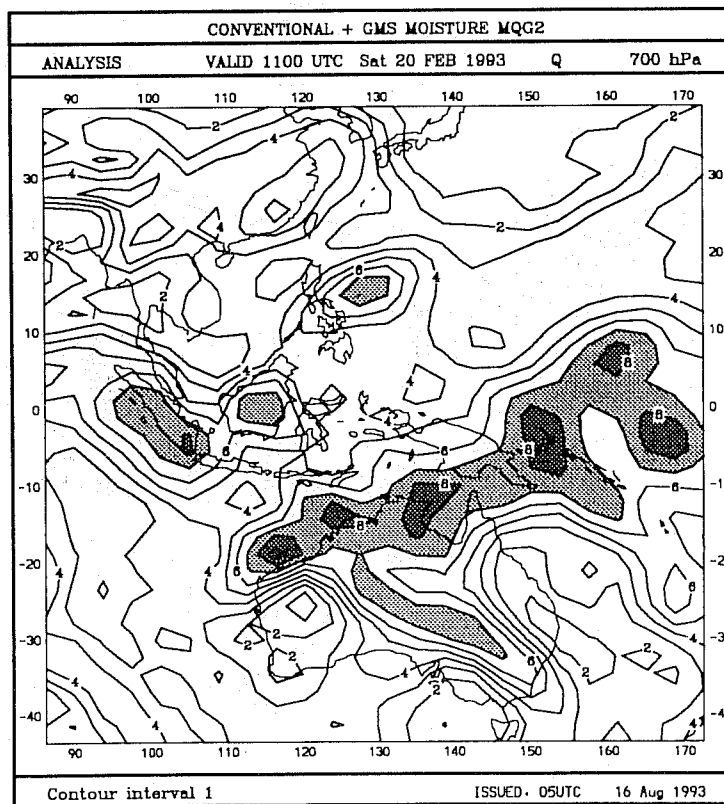
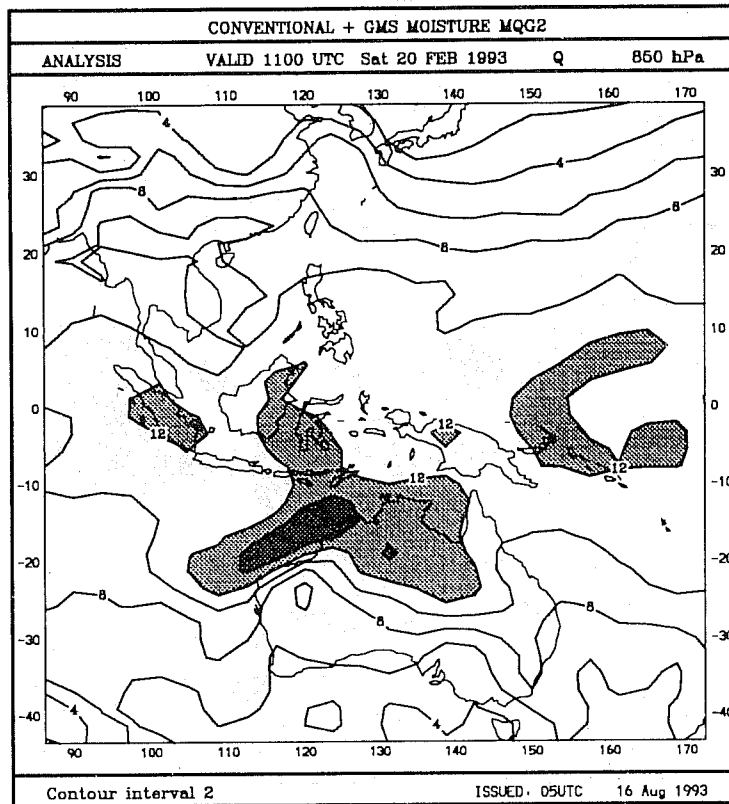


Fig. 20b As in Fig. 20a but conventional + bogus moisture data in new moisture analysis.

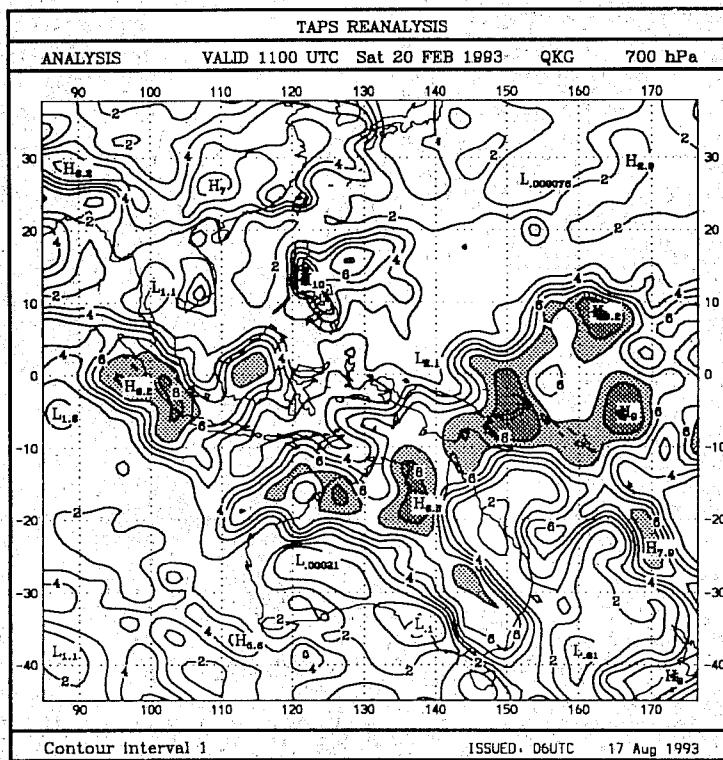
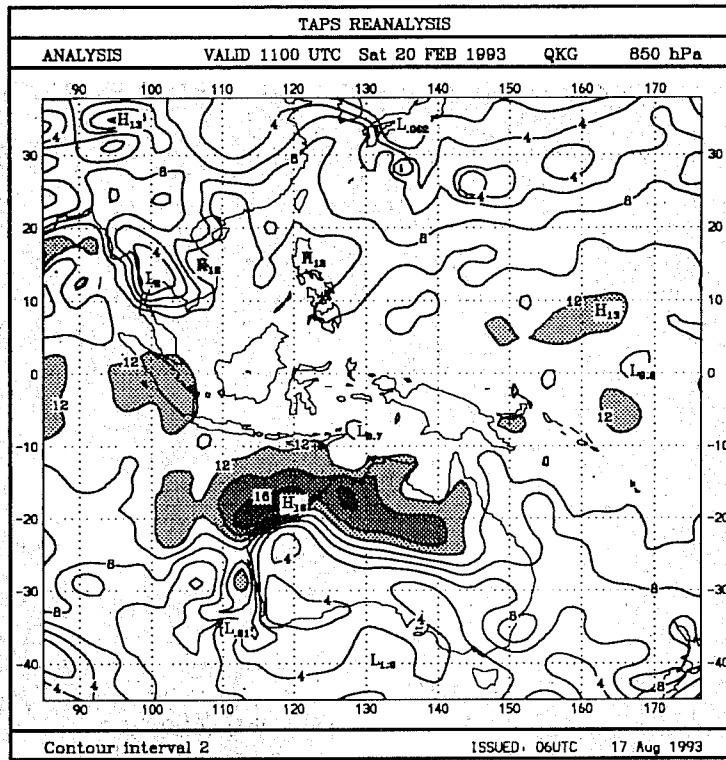


Fig. 20c As in Fig. 20b but from TAPS.



Krishnamurti et al. (1993) have already derived precipitation estimates based on a mix of measurements from OLR, SSM/I and rainguages which in conjunction with physical initialization have resulted in improved nowcasting and one day forecasting skill for precipitation in the FSU model.

The Australian Bureau of Meteorology currently produces daily rainfall analyses operationally. The analysis scheme uses a simple successive correction method with input data from the Australian telegraphic network, which contains some 1250 stations reporting daily. An example of the network and the corresponding analyses are shown in Fig. 22 (the satellite imagery is shown in Fig. 18). The density of the data reflects the population density of Australia, and thus the analyses are less reliable over the interior of Western Australia. In order to make these analyses usable in the modelling systems future work will concentrate on using satellite based estimates to cover these data sparse areas over the continent and the oceans. An example of the satellite estimates for 24 hour periods corresponding to the analysis in Fig. 22 is shown in Fig. 23.

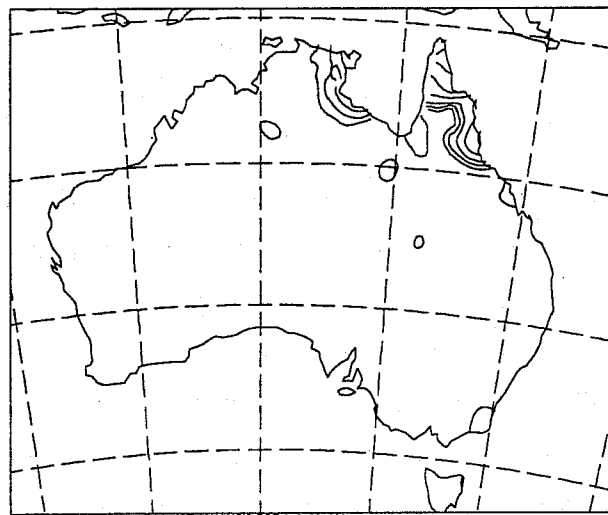
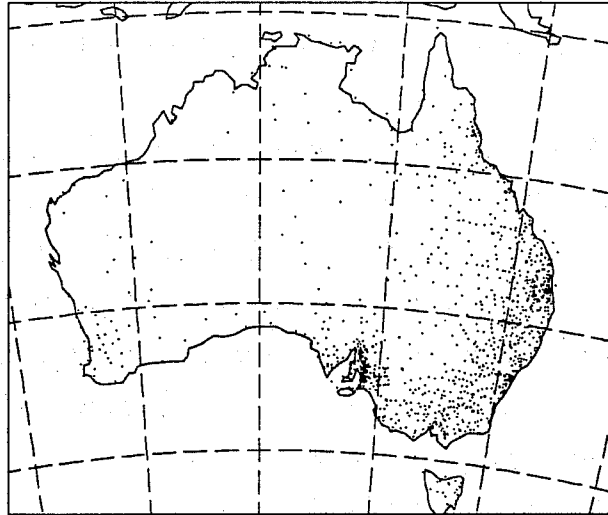
## 6. CONCLUSIONS

A major problem in tropical numerical weather prediction is the inability to adequately represent tropical diabatic forcing in the models. One of the reasons for this is the sparsity of moisture data that often results in poor analysis of the moisture field. Geostationary (and polar-orbiting) satellites such as the GMS provide useful proxy sources of moisture data and diabatic heating. Examples were given to show that such data from GMS has the potential to improve precipitation forecasts, reduce model spin up and possibly provide improved simulation of the Australian summer monsoon. Although the results presented only used GMS data which is currently the only satellite from which synthetic moisture is derived, the coverage could readily be made global if such data were also generated from the other geostationery satellites and made available in real time through the Global Telecommunications Systems (GTS). The procedures for deriving heating rates rely on obtaining reliable estimates of observed precipitation. Global models used at major operational centres have improved significantly in terms of rainfall prediction. Thus, analysis of rainfall using model first guess, conventional rainguage network, and satellite estimates in regions of no data is a feasible option. The results presented show that these analyses could be readily implemented in models and have the potential to improve forecasts in the tropics.

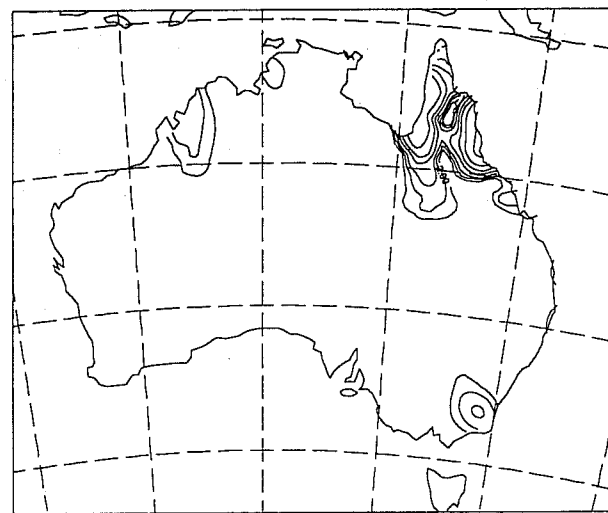
## 7. REFERENCES

Baba, A., 1987: Improvement of the estimation method of moisture data from satellite cloud soundings. JMA/NPD Tech. Rep. No. 16, Japan Meteorological Agency / Numerical Prediction

RAINLIST DATA DISTRIBUTION FOR 940225 1501



RAINLIST ANALYSIS FOR 940130 900



RAINLIST ANALYSIS FOR 940131 900

Fig. 22 Australian rain gauge network (top) and 24-h rainfall analyses valid to 9am (local time) on 30 January (middle) and 31 January 1994 (bottom). Contours plotted are 2, 5, 10, 20, 50, 100 and 200mm.

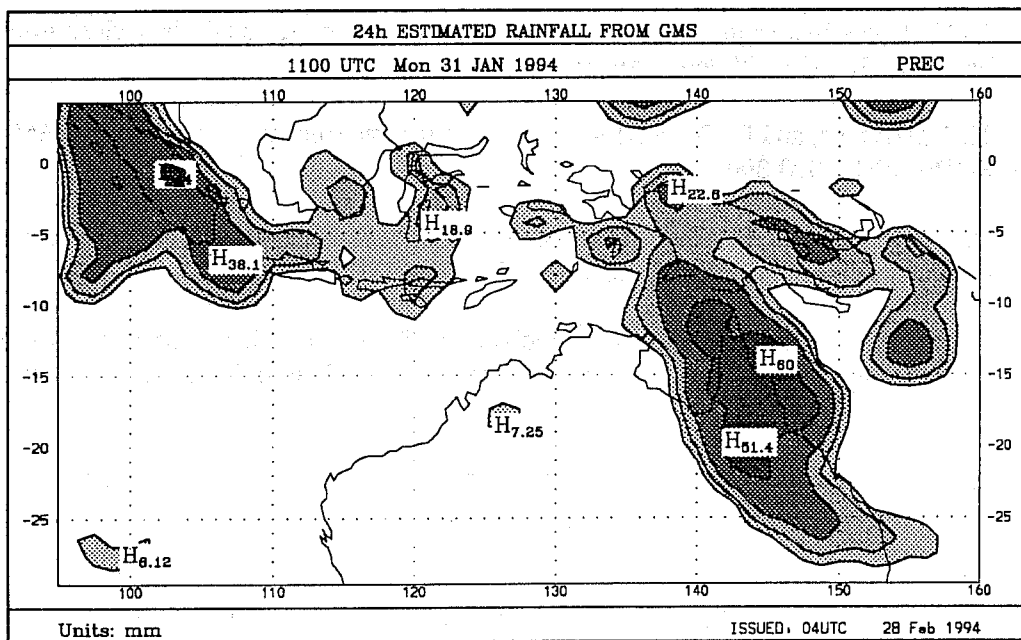
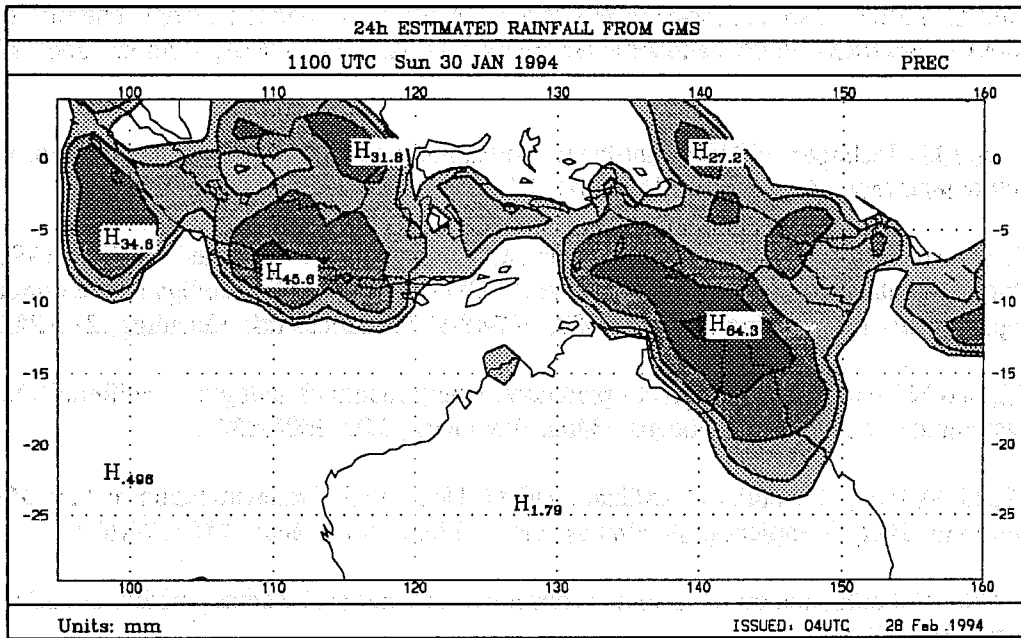


Fig. 23 Satellite estimated rainfall for 24-h periods valid at 1100 UTC 30 January and 31 January 1994.

Division, Tokyo, Japan, 54 pp.

Betts, A.K., and M.J. Miller, 1986: A new convective adjustment scheme. Part II: Single column tests using GATE WAVE, BOMEX, ATEX and Arctic air-mass data sets. *Quart. J. Roy. Meteor. Soc.*, **112**, 693-709.

Bourke, W.P., and J.L. McGregor, 1983: A non-linear vertical mode initialization scheme for a limited area prediction model. *Mon. Wea. Rev.*, **111**, 1749-1771.

Bourke, W.P., R. Seaman, G. Embery, B. McAvaney, M.J. Naughton, T. Hart and L. Rikus, 1990: The BMRC global assimilation and prediction system. ECMWF Seminar Proceedings on Ten years of medium-range weather forecasting, 4-8 Sept 1989, ECMWF, Shinfield Park, Reading, 221-252.

Davidson, N.E., and K. Puri, 1992: Tropical prediction using dynamical nudging, satellite-defined convective heat sources, and a cyclone bogus. *Mon. Wea. Rev.*, **120**, 2501-2522.

Davidson, N.E., J. Wadsley, K. Puri, K. Kurihara, and M. Ueno, 1993: Implementation of the JMA typhoon bogus in the BMRC tropical prediction system. *J. Meteor. Soc. Japan*, **71**, 437-467.

Donner, L.J., 1988: An initialization for cumulus convection in numerical weather prediction models. *Mon. Wea. Rev.*, **118**, 377-385.

Donner, L.J., and P.J. Rasch, 1989: Cumulus initialization in a global model for numerical weather prediction. *Mon. Wea. Rev.*, **117**, 2654-2671.

Fels, S.B., and M.D. Schwarzkopf, 1975: The simplified exchange approximation: A new method for radiative transfer calculations. *J. Atmos. Sci.*, **32**, 1474-1488.

Frank, W.M., and J.L. McBride, 1989: The vertical distribution of heating in AMEX and GATE cloud clusters. *J. Atmos. Sci.*, **46**, 3464-3478.

Guymmer, L.B., 1978: Operational application of satellite imagery to synoptic analysis in the southern hemisphere. Tech. Rep. 26. Bur. Meteor., Australia, 47pp.

Hendon, H.H., N.E. Davidson, and B. Gunn, 1989: Australian summer monsoon onset during AMEX 1987. *Mon. Wea. Rev.*, **117**, 370-390.

Kasahara, A., R.C. Balgovind, and B.B. Katz, 1988: Use of satellite radiometric data for improvement in the analysis of divergent wind in the tropics. *Mon. Wea. Rev.*, **116**, 866-883.

Kasahara, A., and K. Tamiya, 1989: Spin-up of precipitation forecasts with a global atmospheric model. JMA/NPD Tech. Rep. No. 29, Japan Meteorological Agency / Numerical Prediction Division, Tokyo, Japan, 28pp.

Kasahara, A., A.P. Mizzi, and L.J. Donner, 1992: Impact of cumulus initialization on the spinup of precipitation forecasts in the tropics. *Mon. Wea. Rev.*, **120**, 1360-1380.

Krishnamurti, T.N., K. Ingles, S. Cocke, T. Kitade, and R. Pasch, 1984: Details of low latitude medium range numerical weather prediction using a global spectral model. *J. Meteor. Soc. Japan*, **62**, 613-649.

Krishnamurti, T.M., G. Rohally, and H.S. Bedi, 1993: On the improvement of precipitation forecast



- skill from physical initialization. FSU Report No 93-7, Dept. Meteor., Florida State University, Tallahassee, 27pp.
- Kuma, K., 1993: The impact of satellite moisture data upon numerical prediction of Australian monsoon onset. *J. Meteor. Soc. Japan*, **1**, 545-551.
- Kummerow, C., and L. Giglio, 1994: A passive microwave technique for estimating rainfall and vertical structure information from space. Part 1: Algorithm description. *J. App. Meteor.*, **33**, 3-18.
- London, J., 1957: A study of the atmospheric heat balance. Report, Dept. Meteor. and Oceans, New York University, 99pp.
- Mathur, M.B., H.S. Bedi, T.N. Krishnamurti, M. Kanamitsu, and J.S. Woolen, 1992: Use of satellite-derived rainfall for improving tropical forecasts. *Mon. Wea. Rev.*, **120**, 2540-2560.
- Mills, G.A., and N.E. Davidson, 1987: Tropospheric moisture profiles from digital IR satellite imagery: System description and analysis/forecast impact. *Aust. Meteor. Mag.*, **35**, 109-118.
- Olson, W.S., F.S. Fontaine, W.L. Smith, and R.H. Achtor, 1990: Recommended algorithms for the retrievals of rainfall rates in the tropics using SSM/I (DMSP-F8). Manuscript, University of Wisconsin, Madison, 10pp.
- Puri, K., 1987: Some experiments on the use of tropical diabatic heating information for initial state specification. *Mon. Wea. Rev.*, **115**, 1394-1406.
- Puri, K., and M.J. Miller, 1990: The use of satellite data in the specification of convective heating for diabatic initialization and moisture adjustment in numerical weather prediction models. *Mon. Wea. Rev.*, **118**, 67-93.
- Puri, K., N.E. Davidson, L.M. Leslie, and L.W. Logan, 1992: The BMRC tropical limited area model. *Aust. Meteor. Mag.*, **40**, 81-104.
- Puri, K., and N.E. Davidson, 1992: The use of infrared satellite cloud imagery data as proxy data for moisture and diabatic heating in data assimilation. *Mon. Wea. Rev.*, **120**, 2329-2341.
- Puri, K., 1994: Modelling studies on the Australian summer monsoon. To appear in *Mon. Wea. Rev.*
- Rikus, L., 1991: The role of clouds in global climate modelling. BMRC Research Report No. 25, BMRC, Melbourne, 37pp.
- Tiedtke, M., 1987: Parameterization of cumulus convection in large-scale numerical models. *The physical Basis of Climate Modelling*, M.E. Schlesinger, Ed., D. Reidel, 375-431.
- Turpeinen, O.M., 1990: Diabatic initialization of the Canadian regional finite element (RFE) model using satellite data. Part II: Sensitivity to humidity enhancement, latent-heating profile and rain rates. *Mon. Wea. Rev.*, **118**, 1396-1407.
- Turpeinen, O.M., L. Garand, R. Benoit, and M. Roch, 1990: Diabatic initialization of the Canadian regional finite element (RFE) model using satellite data. Part I: Methodology and application to a winter storm. *Mon. Wea. Rev.*, **118**, 1381-1395.
- Wergen, W., 1987: Diabatic nonlinear normal mode initialization for a spectral model with a hybrid vertical coordinate. ECMWF Tech. Rep. No. 59, ECMWF, Shinfield Park, Reading, 83pp.